

LIBRARY  
ROYAL AIRCRAFT ESTABLISHMENT  
BEDFORD.

R. & M. No. 2995  
(15,404)  
A.R.C. Technical Report



MINISTRY OF SUPPLY  
AERONAUTICAL RESEARCH COUNCIL  
REPORTS AND MEMORANDA

# Low-Speed Wind-Tunnel Tests on Two Thin Cranked Wings with 60-deg Sweepback Inboard

By  
C. J. MANSELL

*Crown Copyright Reserved*

LONDON: HER MAJESTY'S STATIONERY OFFICE

1957

SIXTEEN SHILLINGS NET

# Low-Speed Wind-Tunnel Tests on Two Thin Cranked Wings with 60-deg Sweepback Inboard

By

C. J. MANSELL

COMMUNICATED BY THE PRINCIPAL DIRECTOR OF SCIENTIFIC RESEARCH (AIR),  
MINISTRY OF SUPPLY

---

*Reports and Memoranda No. 2995\**  
*April, 1952.*

---

*Summary.*—Low-speed wind-tunnel tests have been made on two thin wings of aspect ratio 3 with 60-deg leading-edge sweep at the root. Both wings show large forward movements of the aerodynamic centre at moderate lift coefficient ( $C_L = 0.5$  to  $0.7$ ). This forward movement can be delayed to  $C_L = 1.0$  by full-span Kruger-type leading-edge flaps. The normal type of split flap with hinge-line parallel to the wing trailing edge gave a decrease in usable  $C_L$  and better results were obtained with flaps with their hinge-line skewed to the wing trailing edge at a smaller angle of sweepback. With skewed split flaps and full-span nose flaps  $C_L = 1.2$  at  $\alpha = 17\frac{1}{2}$  deg was reached on both wings with only small movements of the aerodynamic centre.

Abrupt changes in  $l_v$  and  $n_v$  with change of incidence occurred in the region of flow breakdown on the wing without flaps. These abrupt changes were postponed to  $C_L > 1$  by nose flaps and skewed trailing-edge flaps. Ailerons with unswept hinge-line produced greater rolling moments than ailerons with swept hinge-lines or all-moving tip ailerons.

The Reynolds number of the tests was about  $2.3 \times 10^6$  and the Mach number 0.18. Some favourable scale effects would be expected at higher  $R$ , but the general nature of the breakdown of flow will probably be similar on a full-scale aeroplane.

1. *Introduction.*—Little is known of the stalling characteristics of highly swept-back wings which are suitable for flight at supersonic speeds. Previous wind-tunnel tests have shown that for 60-deg sweepback any wing with an aspect ratio greater than 1.5 is almost certain to suffer from longitudinal instability near the stall. In addition, wing-tip controls are likely to lose their effectiveness as soon as the tip stall commences.

Tests were therefore made on two highly swept-back wings of aspect ratio 3. Their plan-forms represent two designs which are likely to retain good high-speed qualities and yet yield acceptable stalling characteristics. Their thickness/chord ratios are small compared with those in present day use.

The aims of these tests were:

- (a) To investigate how the general character of flow over wings of 60-deg sweepback differed from that over wings with smaller angles of sweepback
- (b) To delay or prevent the onset of longitudinal instability by the addition of nose and trailing-edge flaps
- (c) To determine  $n_v$  and  $l_v$  and aileron effectiveness.

2. *Description of Models and Tests.*—The diagrams of the models are shown in Figs. 1 and 2 and relevant data is given in Tables 1 and 2. Model A had a constant leading-edge sweep and Model B a cranked leading edge. Both models had symmetrical 6 per cent thickness/chord

---

\* R.A.E. Tech. Note Aero. 2158, received 24th November, 1952.

RAE 101 sections (along wind) at the root, thickening to 12 per cent thick at the tip on Model A and 9 per cent thick at the tip on Model B. The models had similar bodies. Model A was also provided with a fin, and a high-set tailplane whose incidence could be altered.

The nose flaps were made of plane sheet metal faired at the leading edge by a small diameter circular tube. They were divided into sections so that the effect of spanwise location might be found.

The nose flaps fitted to Model A were initially flat up to the nose. Plasticine fairings were added to the upper surface of the nose flap (Fig. 3), which delayed the stall by 2 deg incidence as indicated by tufts, and these fairings were retained for all further tests with nose flaps on Model A. Balance measurements showed little change in the overall forces and the nose flaps fitted to Model B were not faired.

Trailing-edge flaps were fitted to both models. On Model A flaps were fitted with hinge-lines both parallel and at an angle to the trailing edge. Owing to their superior performance, only the latter were fitted on Model B. As an alternative to flap-type ailerons, moving-tip ailerons could also be fitted on Model A. Both models were made of mahogany and finished with Phenoglaze. Fig. 3 shows sketches of the trailing-edge flaps and the ailerons which were fitted to Model A.

The Reynolds numbers of the tests were  $2.24 \times 10^6$  and  $2.56 \times 10^6$  for Models A and B respectively. The Mach number of the tests was  $M = 0.18$ .

It was found that the wings twisted in a linear fashion as the lift increased. A maximum of 1 deg decrease of incidence at the tip compared with the root was noted at 30 deg wing incidence on Model A. This twist was thought to have only a small effect on the wing characteristics, and no allowance has been made for it in the results given.

The tunnel corrections applied are the standard ones for unswept wings except for a correction to the pitching moment on the wing due to the variation of the upwash induced by the tunnel walls over the span of the wing. This was calculated from Ref. 1, and was applied as a correction to c.g. position. The correction to incidence and drag calculated from Ref. 1 did not differ appreciably from the standard one for unswept wings. The corrections used due to tunnel constraint were

	$\alpha$ (deg)	$C_D$	$C_m$
Model A	.. .. ..	$0.64C_L$	$0.0116C_L^2$
Model B	.. .. ..	$0.82C_L$	$0.01417C_L^2$

*3. Discussion of Results.—3.1. Model A : Lift, Drag and Pitching Moments.—3.1.1. Without flaps.*—On the wing without the body the lift-curve slope showed an increase in the range of lift coefficient between 0.4 and 0.7 ( $\alpha = 9\frac{1}{2}$  deg and 15 deg). This increase in lift-curve slope was immediately preceded by a marked loss of longitudinal stability at  $C_L = 0.35$  (see Figs. 10 and 11). Coinciding with this loss of stability was an abrupt increase in  $C_{D_0}$  (see Fig. 17). Beyond  $\alpha = 15$  deg the lift-curve slope slowly decreased and this was accompanied by a further loss of longitudinal stability. The addition of the body increased both the initial slope of the lift curve and the longitudinal stability, and also delayed the increase of drag and loss of stability to  $C_L = 0.5$ . Beyond this incidence the curves are roughly parallel to those for the wing alone. Although measurements were continued up to  $\alpha = 27$  deg the wing did not stall completely.

The spanwise lift loading, with and without body, has been calculated by the method of Ref. 2 (Fig. 9). Tests on wings of 0 deg and 40-deg sweep with a similar wing section and Reynolds number suggested that at zero incidence boundary-layer effects should be allowed for by taking a two-dimensional lift slope of 0.92 times the value for potential flow round a thick aerofoil. This factor tends to become smaller with increase of incidence. Unfortunately, in these measurements on 60-deg wings the results do not enable an accurate interpolation of the lift slope at  $\alpha = 0$  deg, but the following table compares the calculated value at  $\alpha = 0$  deg with the measured

value of  $C_L/\alpha$  at  $\alpha = 6$  deg. The effect of the body is of the order predicted, and the difference between the calculated and measured overall values may be due to increased boundary-layer effects on the 60-deg wing.

TABLE A

	$\frac{C_L}{\alpha(\text{radn})}$ Measured $\alpha = 6$ deg	$\frac{C_L}{\alpha(\text{radn})}$ Calculated $\alpha = 0$ deg
Wing alone .. ..	2.40	2.65
Wing and body .. ..	2.70	2.87*

\* This includes an estimated 0.02 due to lift on the tail of the body.

The character of the flow over the wing was investigated both by use of silk tufts and by spreading a thin layer of thick white oil on the wing and observing the ensuing pattern with wind on. Between  $\alpha = 4$  deg and 5 deg a thin line of oil was retained at the leading edge on the upper surface along the whole of the semi-span except for a small proportion where the wing thickness was a maximum. This was interpreted as evidence of a laminar separation with turbulent re-attachment, a line of oil being retained in the region of the laminar separation. At  $\alpha = 10\frac{1}{2}$  deg a violent eddying started from the leading edge at about 60 per cent semi-span from the centre of the wing. The surface tufts also showed a disturbance starting near this point. As the incidence was increased further a wedge of oil, triangular in shape, was formed, the apex moving towards the body until at  $\alpha = 18.7$  deg it had reached the wing leading-edge-body junction as shown in Fig. 4a. Oil was swept into this triangle from the leading edge and inboard parts of the wing and drifted slowly towards the tip.

Figs. 6, 7 and 8 are diagrams of the deep tufts compiled from photographs. At  $\alpha = 9.4$  deg tufts at the surface near the trailing edge showed slight boundary-layer outflow. At  $\alpha = 10.5$  deg however tufts at the surface near the leading edge indicated that the component of flow normal to the leading edge was reversed while tufts 3.30 in. above the surface were inclined slightly inboard. At  $\alpha = 18.7$  deg, Fig. 8 shows that this type of flow extended inboard and became intensified. Pronounced reversal of flow occurred as far back as 50 per cent chord on the surface at section C and tufts above the surface showed large inclinations of the flow towards the body.

The evidence of oil and tufts showed that a sharply defined vortex was present over the upper surface of the wing at all incidences above 12 deg. It originated at the wing leading edge and was swept downstream above and slightly behind the triangular accumulation of oil (Fig. 4c). This vortex had the same direction of rotation as a normal trailing vortex and left the wing trailing edge well inboard of the tip. A weaker vortex of opposite sense was detected over the wing-body junction also springing from the leading edge. The surface tufts in Fig. 5 show flow directions consistent with the presence of a vortex above the upper surface and lines have been drawn on the photographs of the tufts indicating the probable limits wherein the vortex lay.

Wings of more moderate sweepback and larger thickness/chord ratios do not have this type of vortex flow. It may be associated with the stalling characteristics of thin aerofoils. For example, Ref. 3 shows that on a 6 per cent thick unswept aerofoil the stall occurs as a result of a laminar separation and a re-attachment, which starts at low incidence ( $\alpha = 5$  deg) at the leading edge. The point of re-attachment moves back until just before the stall, the separated region extends over 40 per cent chord from the leading edge. In contrast, on 12 per cent and 9 per cent thick aerofoils the laminar separation remains very small in chordwise extent right up to the stall (Ref. 4). On a swept wing the large region of separated flow and re-attachment would produce a vortex type of flow similar to that described above.

The changes in slope of the lift, drag and pitching-moment curves occur at  $\alpha = 10.5$  deg when the sudden enlargement of the leading-edge separation takes place and the associated vortex appears above the surface. The presence of the vortex thus has the effect of modifying the spanwise load distribution so that a slight increase in overall lift-curve slope is accompanied by a forward movement of the aerodynamic centre.

**3.1.2. The effect of trailing-edge flaps and nose flaps.**—A normal swept flap with a hinge-line parallel to the trailing edge was fitted to Model A initially. This flap caused a decrease in the lift slope amounting to a loss of 0.16 in lift coefficient at  $\alpha = 25$  deg and did not delay longitudinal instability at all (see Fig. 12). A split flap was then fitted whose hinge-line was skewed to the trailing edge so that the angle of sweep of the hinge-line was reduced. This had a remarkably beneficial effect on the pitching-moment curve, the unstable kink in the curve being delayed to  $C_L = 0.8$  (Fig. 16). All further tests with various combinations of nose flaps and trailing-edge flaps on both models were made with this type of flap.

Full-span nose flaps delayed the longitudinal instability by about 10 deg incidence to a  $C_L = 1.0$  without trailing-edge flaps and  $C_L = 1.2$  with trailing-edge flaps down (Figs. 14 and 16). Part-span nose flaps either outboard or inboard were not very effective in delaying the longitudinal stability. As the nose flaps used were of the Kruger extensible type they caused a forward movement of the aerodynamic centre at low incidence. Drooped nose flaps which do not extend the wing chord would not do this, though they might not be so effective in increasing the incidence at which the breakdown of flow occurs.

Curves of effective profile drag show the effect of separation clearly and how it is delayed by full-span nose flaps (Fig. 17).

**3.2. Model B : Lift Drag and Pitching Moments.**—**3.2.1. Without flaps.**—On Model B the pitching-moment curves (Fig. 19) show an increase in stability above  $C_L = 0.4$ . This initial increase in stability is accompanied by an increase in lift slope. It is associated with a separation of the air flowing from bottom to top surface round the tip of the wing and with a consequent modification to the trailing vortex pattern at the tip. The vorticity leaving the tip is distributed along the tip chord and forms a vertical trailing sheet, which causes an increase in the local span loading. There is thus an increase in the overall lift-curve slope which, in the case of a swept-back wing, is accompanied by an increase in stability. The drag starts increasing rapidly at about  $C_L = 0.5$  just after the lift slope increase starts. This modification to the tip vortex has its largest effect on untapered wings, and on Model A with its very small tip chord it has no appreciable effect.

At  $C_L = 0.6$  a separation begins from near the leading edge at the crank. This spreads and at  $C_L = 0.7$  causes the aerodynamic centre to move forward. At higher incidences the separation moves right inboard and the flow becomes very similar to that on Model A.

**3.2.2. The effects of trailing-edge flaps and nose flaps.**—Nose flaps extending from 58 per cent to 92 per cent of the semi-span eliminate the increasing stability but do not change the  $C_L$  at which the instability occurs. Full-span nose flaps increase this usable  $C_L$  to about 0.95 without flaps and to about 1.2 with trailing-edge flaps (Figs. 19 and 21).

Detailed comparisons of Models A and B are shown in Figs. 23 and 24. Without flaps Model B has rather better characteristics, the longitudinal instability being delayed by about  $C_L = 0.2$ , but with nose flaps and trailing-edge flaps there is very little to choose between the pitching-moment curves. Model A gives a higher  $C_{L\max}$ , but this is well above the usable  $C_L$ .

**3.3. The Measurement of Downwash and the Effect of a Tailplane on Model A.**—The few tests made on Model A with tailplane showed similar pitching-moment curves to those without a tailplane (Fig. 25). Longitudinal instability occurred at about the same value of lift coefficient though the change in stability was generally rather greater with the tail. Curves of downwash (Fig. 26) shows that this was due to the increase in downwash when the vortex was first formed  $d\varepsilon/d\alpha$  increasing from about 0.25 at low incidence to over 1 above  $\alpha = 17$  deg. Nose flaps delay the increase in  $d\varepsilon/d\alpha$  to a higher incidence.

**3.4. Lateral and Directional Stability.**—For both models —  $l_v$  varies almost linearly with  $C_L$  at low coefficients while the slope of the  $n_v$  curve increases slightly with incidence (Figs. 27 and 28). As the incidence is increased at a constant angle of sideslip, tuft studies showed that the rear wing stalled first over the outer region, producing a sharp drop in —  $n_v$ , but with little effect on  $l_v$ . A few degrees later the forward wing stalled as well, —  $l_v$  at first remaining constant and then beginning to fall off, while  $n_v$  increases again. A similar sequence of events occurs with various combinations of flaps. At the higher incidences the curves of rolling and yawing moments are not linear with angle of sideslip (Fig. 29),  $n_v$  in particular tending to have a larger value near the origin than the average value for  $\beta = \pm 5$  deg as given in Fig. 28. With full-span nose flaps —  $l_v$  reaches very high values, 0·3 being attained on both models.

**3.5. Aileron Effectiveness.**—Fig. 30 and 31 show the ability of the flap-type ailerons to hold the adverse roll due to sideslip. On Model A the ailerons (20 deg up port and 10 deg down starboard) will hold 10 deg of sideslip at  $C_L = 0\cdot8$  without flaps, but with nose flaps and trailing-edge flaps at the same incidence ( $C_L = 1\cdot15$ ) they will only balance 6 deg sideslip. On Model B the same aileron angles will only balance  $4\frac{1}{2}$  deg sideslip at  $C_L = 1\cdot05$ . This difference is due to the smaller effectiveness of the ailerons with a swept-back hinge-line as on Model B. The ratio of aileron area over wing area is nearly the same for the two models but the rolling moment produced on Model B is only 70 per cent of that on Model A at low incidence and falls to only 50 per cent at high incidence. Nose flaps reduce the drop of rolling moment with incidence especially for the large angles of an upgoing aileron.

The all-moving tip-type ailerons (area 17 per cent higher than the area of the flap-type ailerons) have a much smaller effectiveness. At high  $\alpha$  the tip with increased incidence gives little rolling moment and differential movement would be an advantage. The values of aileron effectiveness are shown in the table below.

TABLE B  
For two Ailerons (Mean for  $\xi = + 10$  deg)

Model	Aileron	$\frac{dC_t}{d\xi} \times 10^3/\text{radn}$		
		No flaps		With nose flaps
		$C_L = 0$	$C_L = 0\cdot8$	$C_L = 0\cdot8$
A	Flap-type .. ..	1·62	1·24	1·29
B	Flap-type .. ..	1·09	0·65	—
A	All-moving tip ..	1·02	0·80	—

**4. Conclusions.**—(a) Tests on two thin wings of 60-deg leading-edge sweep at the root but with different plan-forms have shown that a marked longitudinal instability starts at  $C_L = 0\cdot5$  and  $0\cdot7$  respectively, on the wings with fuselage but without flaps. The wing with reduced leading-edge sweep at the tip has better characteristics than the wing with reduced sweep only on the trailing edge. The early change in stability is associated with the formation of a vortex type of flow, above the wing surface, which is characteristic of thin and highly swept wings

(b) Part-span Kruger-type nose flaps either inboard or outboard have little effect on the value of  $C_L$  at which instability starts, but full-span nose flaps give an appreciable increase

(c) Normal split flaps with hinge-line parallel to the wing trailing edge give a decrease in maximum usable  $C_L$  but flaps with a skewed hinge-line of reduced sweep give an appreciable increase. With full-span nose flap and part-span trailing-edge flap of this type, a  $C_L$  of 1.2 could be achieved on both wings before the pitching-moment curves became unstable

(d) A few measurements made on one of the wings with a high tailplane show longitudinal instability occurring at about the same  $C_L$  as without tailplane. When the breakdown of flow occurs there is a larger change of stability on the model with tailplane due to the large increase in downwash at the tail

(e) Appreciable erratic changes in  $l_v$  and  $n_v$  also occur on the wing and fuselage without flaps at moderate  $C_L$ , while with full-span nose flaps and trailing-edge flaps  $l_v$  varies linearly with  $C_L$ . With this flap configuration, the slope of the  $n_v$  curve for Model A increases slightly with  $C_L$  up to  $C_L = 1.2$  where there is a sudden fall in the value of  $n_v$ . The value of  $l_v$  is then -0.3. On Model B the rapid change in  $n_v$  occurs at  $C_L = 0.7$

(f) The wing with aileron hinge-line normal to the wind direction produces a larger rolling moment than one with a swept hinge-line, and also more than an all-moving tip aileron.

*Acknowledgment.*—The author wishes to acknowledge the assistance of Miss M. Whittaker in wind-tunnel work and the preparation of this report.

#### LIST OF SYMBOLS

$A$	Wing aspect ratio
$b$	Wing span
$c$	Local wing chord
$\bar{c}$	Wing mean chord ( $= S/b$ )
$C_D$	Drag coefficient ( $= \text{drag}/\frac{1}{2}\rho U^2 S$ )
$C_{D_0}$	Profile-drag coefficient ( $= C_D - C_L^2/\pi A$ )
$C_L$	Lift coefficient ( $= \text{lift}/\frac{1}{2}\rho U^2 S$ )
$\bar{C}_L$	Total lift in Fig. 9
$C_i$	Rolling-moment coefficient ( $= \text{rolling moment}/\frac{1}{2}\rho U^2 S b$ )
$C_m$	Pitching-moment coefficient ( $= \text{pitching moment}/\frac{1}{2}\rho U^2 S \bar{c}$ )
$C_m'$	Pitching-moment coefficient transferred to different c.g. position (see figures and tables)
$C_n$	Yawing-moment coefficient ( $= \text{yawing moment}/\frac{1}{2}\rho U^2 S b$ )
$C_y$	Side-force coefficient ( $= \text{side force}/\frac{1}{2}\rho U^2 S$ )
$l_v$	$= dC_i/d\beta$ ( $\beta$ in radians)
$n_v$	$= dC_n/d\beta$ ( $\beta$ in radians)
$S$	Wing gross area
$U$	Main-stream wind speed
$y$	Spanwise position
$y_v$	$= \frac{1}{2}dC_y/d\beta$ ( $\beta$ in radians)
$\alpha$	Wing incidence (degrees)
$\beta$	Angle of sideslip (normally degrees)
$\varepsilon$	Mean angle of downwash at the tailplane (degrees)
$\xi$	Angle of deflection of aileron (degrees)
$\eta_T$	Angle of tailplane setting relative to wing chord (degrees)
$\rho$	Main-stream air density

## REFERENCES

No.	Author	Title, etc.
1	W. E. A. Acum .. .. ..	Corrections for symmetrical swept and tapered wings in rectangular wind tunnels. R. & M. 2777. April, 1953.
2	D. Küchemann .. .. ..	A simple method of calculating the wing and chordwise loading on thin swept wings. R.A.E. Report Aero 2392. A.R.C. 13,758. August, 1950.
3	G. B. McCullough and D. E. Gault	Boundary-layer and stalling characteristics of the NACA 64A006 airfoil section. N.A.C.A. Tech. Note 1923. August, 1949. (A.R.C. 12, 781.)
4	D. E. Gault .. .. ..	Boundary layer and stalling characteristics of the NACA 63-009 airfoil section. N.A.C.A. Tech. Note 1894. 1949.

TABLE 1

*Model Data Model A*

*Wing*

Wing span, $b$ .. .. .. .. .. .. .. .. ..	64.00 in.
Mean chord, $\bar{c}$ .. .. .. .. .. .. .. .. ..	21.36 in.
Aspect ratio, $A$ .. .. .. .. .. .. .. .. ..	3
Leading-edge sweepback (constant over whole span) .. .. .. .. .. .. .. .. ..	60 deg
Quarter-chord sweepback $\left\{ \begin{array}{l} y = 0 \text{ to } 0.549 b/2 \\ y = 0.549 b/2 \text{ to } 1.00 b/2 \end{array} \right.$ .. .. .. .. .. .. .. .. ..	60 deg
Wing area, $S$ .. .. .. .. .. .. .. .. ..	52.4 deg
Thickness/chord ratio .. .. .. .. .. .. .. .. ..	1368 in. <sup>2</sup>
Dihedral .. .. .. .. .. .. .. .. ..	see Table 3
Distance of mean quarter-chord point from wing apex along centre-line .. .. .. .. .. .. .. .. ..	0 deg
Root chord .. .. .. .. .. .. .. .. ..	29.20 in.
Chord, section A-A ( $y = 0.549 b/2$ ) .. .. .. .. .. .. .. .. ..	27.00 in.
Chord, section B-B ( $y = 0.75 b/2$ ) .. .. .. .. .. .. .. .. ..	27.00 in.
Tip chord .. .. .. .. .. .. .. .. ..	15.86 in.
	2.03 in.

*Ailerons*

Dimensions .. .. .. .. .. .. .. .. ..	see Fig. 3b
Flap type : Area aft of hinge/Wing area .. .. .. .. .. .. .. .. ..	0.0895
All-moving tip type : Area tip/Wing area .. .. .. .. .. .. .. .. ..	0.104

*Nose flaps*

Chord along wind and along nose flap (constant over whole span) .. .. .. .. .. .. .. .. ..	2.16 in.
Nose flap chord/Wing root chord .. .. .. .. .. .. .. .. ..	0.08
Angle of droop to chord-line (normal to leading edge) .. .. .. .. .. .. .. .. ..	50 deg
Span $\left\{ \begin{array}{l} \text{Nose flap (1)} .. .. .. .. .. .. .. .. .. \\ \text{Nose flap (2)} .. .. .. .. .. .. .. .. .. \end{array} \right.$ .. .. .. .. .. .. .. .. ..	$y = 0.109 b/2 \text{ to } 0.312 b/2$
	$y = 0.312 b/2 \text{ to } 0.907 b/2$

*Trailing-edge flaps*

Span .. .. .. .. .. .. .. .. ..	Flap (1)	Flap (2)
Trailing-edge flap chord/Local wing chord .. .. .. .. .. .. .. .. ..	$0.109 b/2 \text{ to } 0.549 b/2$	$0.109 b/2 \text{ to } 0.549 b/2$
	0.30	0.30
Position of hinge of trailing-edge flap when extended .. .. .. .. .. .. .. .. ..	$0.70 c \left\{ \begin{array}{l} \text{inboard} \\ \text{and} \\ \text{outboard} \end{array} \right.$	$1.00 c \text{ inboard}$
Angle of flap to chord-line about hinge-line .. .. .. .. .. .. .. .. ..	60 deg	$0.70 c \text{ outboard}$
		60 deg

*Tailplane*

Area .. .. .. .. .. .. .. .. ..	337 in. <sup>2</sup>
Mean chord .. .. .. .. .. .. .. .. ..	11.62 in.
Aspect ratio .. .. .. .. .. .. .. .. ..	2.53
Span .. .. .. .. .. .. .. .. ..	29.15 in.
Sweep of quarter-chord line .. .. .. .. .. .. .. .. ..	42 deg 29 min
Distance of tail apex aft of wing apex .. .. .. .. .. .. .. .. ..	46.90 in.
Distance of tail apex above body centre-line .. .. .. .. .. .. .. .. ..	6.95 in.

TABLE 2

## Model Data Model B

## Wing

Wing span, $b$	..	..	..	..	..	..	..	..	..	72.00 in.
Mean chord, $\bar{c}$	..	..	..	..	..	..	..	..	..	24.21 in.
Aspect ratio, $A$	..	..	..	..	..	..	..	..	..	3.00
Leading-edge sweepback	$y = 0$ to $0.584 b/2$	..	..	..	..	..	..	..	..	59 deg
	$y = 0.584 b/2$ to $0.916 b/2$	..	..	..	..	..	..	..	..	48.50 deg
Quarter-chord sweepback	$y = 0$ to $0.584 b/2$	..	..	..	..	..	..	..	..	57.1 deg
	$y = 0.584 b/2$ to $0.916 b/2$	..	..	..	..	..	..	..	..	45.3 deg
Wing area, $S$	..	..	..	..	..	..	..	..	..	1743 in. <sup>2</sup>
Thickness/chord ratio	..	..	..	..	..	..	..	..	..	see Table 3
Dihedral	..	..	..	..	..	..	..	..	..	0 deg
Distance of mean quarter-chord point aft of wing apex along centre-line	..	..	..	..	..	..	..	..	..	31.70 in.
Root chord	..	..	..	..	..	..	..	..	..	33.00 in.
Chord, section A-A ( $y = 0.584 b/2$ )	..	..	..	..	..	..	..	..	..	23.00 in.
Chord, section B-B ( $y = 0.916 b/2$ )	..	..	..	..	..	..	..	..	..	17.00 in.
Tip dimensions	..	..	..	..	..	..	..	..	..	see below

## Ailerons

Root chord	..	..	..	..	..	..	..	..	..	5.75 in.
Tip chord	..	..	..	..	..	..	..	..	..	3.875 in.
Area/Wing area	..	..	..	..	..	..	..	..	..	0.083

## Nose flaps

Chord normal to leading edge and along nose flap	$y = 0.097 b/2$ to $0.584 b/2$	..	..	..	..	..	..	..	..	1.37 in.
	$y = 0.584 b/2$ to $0.916 b/2$	..	..	..	..	..	..	..	..	1.50 in.
Angle of droop to chord line (normal to leading edge)	$y = 0.097 b/2$ to $0.584 b/2$	..	..	..	..	..	..	..	..	56 deg 52 min
	$y = 0.584 b/2$ to $0.916 b/2$	..	..	..	..	..	..	..	..	50 deg
Span	Nose flap (1) ..	..	..	..	..	..	..	..	..	$y = 0.097 b/2$ to $0.278 b/2$
	Nose flap (2) ..	..	..	..	..	..	..	..	..	$y = 0.278 b/2$ to $0.584 b/2$
	Nose flap (3) ..	..	..	..	..	..	..	..	..	$y = 0.584 b/2$ to $0.916 b/2$

## Trailing-edge flaps

Span	..	..	..	..	..	..	..	..	..	$y = 0.097 b/2 - 0.584 b/2$
Trailing-edge flap chord/Local wing chord	..	..	..	..	..	..	..	..	..	0.30
Position of hinge of trailing-edge flap when extended	..	..	..	..	..	..	..	..	..	{ 1.00 c inboard
Angle of flap to chord-line about hinge-line	..	..	..	..	..	..	..	..	..	0.70 c outboard

## Wing tip co-ordinates

	chordwise (in.)	spanwise (in.)
	2.865	0.05
	3.971	0.10
	5.455	0.20
	6.530	0.30
	8.121	0.50
	9.312	0.70
	10.682	1.00
	12.328	1.50
	13.500	2.00
	14.370	2.50
	15.025	3.00

## C.G. positions for pitching moments (unless otherwise stated on graph or table)

Model A without tail	..	..	..	..	..	..	..	..	..	0.30 $\bar{c}$
Model A with tail	..	..	..	..	..	..	..	..	..	0.42 $\bar{c}$
Model B without tail	..	..	..	..	..	..	..	..	..	0.28 $\bar{c}$

## C.G. positions for rolling and yawing moments

Model A	..	..	..	..	..	..	..	..	..	0.52 $\bar{c}$
Model B	..	..	..	..	..	..	..	..	..	0.283 $\bar{c}$
All c.g.'s on wing chord-line	..	..	..	..	..	..	..	..	..	

TABLE 3  
*Co-ordinates of Aerofoil Section used on Both Models*

RAE 101 6 per cent thick

Distance from leading edge (per cent $c$ )	Ordinate (per cent $c$ )	Section		Model A	Model B		
				$\frac{y}{b/2}$	per cent thick	$\frac{y}{b/2}$	per cent thick
0·50	0·519						
0·75	0·641						
1·25	0·819						
2·50	1·152						
5·00	1·596						
7·50	1·915						
10·0	2·163						
15·0	2·530						
20·0	2·781						
25·0	2·930	Centre-line ..	0	6	0	6	
30·0	3·000						
35·0	2·970	A-A ..	0·55	6	0·584	7·5	
40·0	2·882						
45·0	2·741	B-B ..	0·75	12	—	—	
50·0	2·559						
55·0	2·352	Tip ..	1·00	12	0·825	9	
60·0	2·119						
65·0	1·870						
70·0	1·611						
75·0	1·341						
80·0	1·070						
85·0	0·811						
90·0	0·541						
95·0	0·270						
100·0	0						

Leading-edge radius  
0·274 per cent  $c$

*Note : Leading-edge radius is proportional to the square of the thickness/chord ratio.*

TABLE 4  
*Co-ordinates of Body used on Both Models*

Distance from nose (in.)	Radius (in.)
1·00	1·526
2·00	2·062
3·00	2·479
4·00	2·800
5·00	3·031
6·00	3·203
7·00	3·339
8·00	3·429
9·00	3·487
10·00	3·500
65·00	3·500
80·00	1·000
81·00	0
Nose radius ..	1·30
Tail radius ..	1·00

	Model A	Model B
Body nose to wing apex .. .. ..	10·0 in.	12·5 in.
Body symmetrical about wing plane on both models.		

TABLE 5

Model A. Effect of Nose Flaps and Trailing-Edge Flaps

$$c.g. \begin{cases} 0.52 \bar{c} \\ 0.30 \bar{c} \end{cases} \quad \begin{matrix} C_m \\ C_{m'} \end{matrix}$$

\*Wing alone

$\alpha$	$C_L$	$C_D$	$C_m$	$C_{m'}$
0.1	-0.002	0.0089	+0.0013	+0.0017
2.2	+0.099	0.0114	0.0194	-0.0024
4.25	0.175	0.0150	0.0365	-0.0022
5.25	0.219			
6.3	0.263	0.0204	0.0539	-0.0043
7.3	0.304	0.0235	0.0624	-0.0046
8.35	0.348	0.0269	0.0704	-0.0062
9.35	0.389	0.0369	0.0835	-0.0023
10.4	0.432	0.0501	0.0959	+0.0004
11.45	0.481	0.0684	0.1088	0.0021
12.45	0.538	0.0890	0.1248	0.0049
13.5	0.592	0.1121	0.1439	0.0114
14.55	0.656	0.1415	0.1613	0.0137
18.65	0.827	0.2408	0.2323	0.0428
20.7	+0.911	0.3020	+0.2801	+0.0690

Wing and fuselage and nose flap (1)

$\alpha$	$C_L$	$C_D$	$C_m$	$C_{m'}$
0	0.017	0.0157	-0.0039	-0.0079
2.05	0.095	0.0147	+0.0116	-0.0094
4.1	0.188	0.0161	0.0314	-0.0101
8.25	0.393	0.0277	0.0735	-0.0130
10.3	0.485	0.0466	0.0973	-0.0097
12.35	0.560	0.0754	0.1194	-0.0047
14.45	0.669	0.1230	0.1645	+0.0151
16.5	0.781	0.1742	0.1837	0.0081
18.55	0.892	0.2390	0.2166	0.0136
20.6	0.971	0.2917	0.2439	0.0211
22.65	1.046	0.3540	+0.2795	+0.0368

Wing and fuselage alone

$\alpha$	$C_L$	$C_D$	$C_m$	$C_{m'}$
0.15	0.018	0.0088	+0.0041	0
4.25	0.200	0.0145	0.0381	-0.0059
6.3	0.309	0.0228	0.0557	-0.0121
8.35	0.391	0.0293	0.0727	-0.0135
9.4	0.453	0.0356	0.0813	-0.0186
10.45	0.500	0.0441	0.0810	-0.0195
11.45	0.550	0.0677	0.1073	-0.0142
12.5	0.623	0.1016	0.1338	-0.0046
16.65	0.840	0.2060	0.2036	+0.0139
20.75	0.986	0.3328	0.2740	0.0448
24.85	1.117	0.4715	0.3450	0.0787
25.85	1.142	0.5061	0.3579	0.0829
26.85	1.171	0.5463	+0.3702	+0.0860

Wing and fuselage and nose flap (2)

$\alpha$	$C_L$	$C_D$	$C_m$	$C_{m'}$
0.15	0.012	0.0222	-0.0064	-0.0091
4.25	0.221	0.0211	+0.0424	-0.0066
8.4	0.425	0.0358	0.0897	-0.0038
10.45	0.521	0.0492	0.1125	-0.0021
14.55	0.694	0.0994	0.1590	+0.0055
16.65	0.804	0.1488	0.1904	0.0112
20.75	0.991	0.2694	0.2535	0.0285
24.9	1.180	0.4283	+0.3563	+0.0808

\* Only test without fuselage.

TABLE 5—*continued*

Nose flaps (1) and (2)

$\alpha$	$C_L$	$C_D$	$C_m$	$C_m'$	$C_t$	$C_n$	$C_y$
0	-0.018	0.0292	-0.0229	-0.0190	+0.42	+0.13	+7.88
4.1	+0.186	0.0225	+0.0312	-0.0100	-0.63	0	+1.80
8.25	0.388	0.0317	0.0830	-0.0022	-0.47	-0.21	0
12.35	0.584	0.0576	0.1321	+0.0037	-0.34	-0.09	+1.13
14.45	0.692	0.0820	0.1529	+0.0009	-0.13	-0.13	+1.13
16.5	0.775	0.1069	0.1720	+0.0015	-0.04	-0.13	+0.45
18.55	0.874	0.1468	0.1978	+0.0048	0	+0.47	-1.13
20.65	0.997	0.2157	0.2205	-0.0020	+1.10	+0.97	-5.63
22.7	1.104	0.3023	0.2708	+0.0184	+0.42	-0.30	-1.58
24.75	1.184	0.3861			-0.59	-0.13	-4.05
26.8	1.243				-0.55	-0.13	-4.05
29.2	1.288						
30.85	+1.346						

Trailing-edge flaps (2)

$\alpha$	$C_L$	$C_D$	$C_m$	$C_m'$
-7.8	0.082	0.0973	-0.0772	-0.0946
-3.7	0.260	0.0959	-0.0462	-0.1021
+0.4	0.456	0.1056	-0.0105	-0.1109
2.45	0.542	0.1188	+0.0074	-0.1127
4.55	0.649	0.1247	0.0242	-0.1202
8.65	0.836	0.1693	0.0624	-0.1246
9.7	0.890	0.1936	0.0790	-0.1213
10.7	0.929	0.2116	0.0902	-0.1193
11.75	0.992	0.2548	0.1235	-0.1011
12.8	1.047	0.2909	0.1462	-0.0921
13.8	1.092	0.3193	0.1612	-0.0886
14.85	1.151	0.3557	0.1994	-0.0851
16.9	1.225	0.4079	0.2030	-0.0807
18.95	1.329	0.4921	0.2389	-0.0728
21.05	1.417	0.5755	0.2731	-0.0629
23.05	1.478	0.6536	0.3079	-0.0478
+25.05	1.464	0.7251	+0.3553	-0.0031

Trailing-edge flaps (2). Nose flaps (1)

$\alpha$	$C_L$	$C_D$	$C_m$	$C_m'$
0.25	0.425	0.0979	-0.0176	-0.1111
4.4	0.605	0.1133	+0.0184	-0.1162
8.5	0.800	0.1520	0.0634	-0.1156
10.55	0.895	0.1945	0.0797	-0.1218
12.65	1.005	0.2472	0.1268	-0.1009
14.7	1.086	0.2958	0.1542	-0.0935
16.75	1.178	0.3598	0.1839	-0.0872
18.8	1.252	0.4251	0.2108	-0.0802
20.85	1.350	0.5039	0.2375	-0.0796
22.9	1.435	0.5815	0.2673	-0.0735
24.95	1.482	0.6564	+0.2920	-0.0648
25.95	1.490			

TABLE 5—*continued*

Trailing-edge flaps (2). Nose flaps (2)

$\alpha$	$C_L$	$C_D$	$C_m$	$C_m'$
-3.7	0.249	0.1075	-0.0547	-0.1074
+0.4	0.454	0.1110	-0.0085	-0.1084
2.45	0.546	0.1169	+0.0132	-0.1078
4.55	0.650	0.1272	0.0377	-0.1067
8.65	0.838	0.1573	0.0832	-0.1043
9.7	0.882	0.1709	0.0931	-0.1044
10.7	0.934	0.1805	0.1048	-0.1047
11.75	0.989		0.1177	-0.1060
12.8	1.027	0.2093	0.1292	-0.1013
13.8	1.069	0.2264	0.1415	-0.0987
14.85	1.133	0.2460	0.1552	-0.1001
16.9	1.213	0.3117	0.1873	-0.0877
18.95	1.311	0.3912	0.2209	-0.0802
21.0	1.390	0.4990	0.2910	-0.0340
23.05	1.461	0.5846	0.3318	-0.0142
+25.1	1.493	0.6710	+0.3767	+0.0178

Trailing-edge flaps (2). Nose flaps (1) and (2)

$\alpha$	$C_L$	$C_D$	$C_m$	$C_m'$	$C_l$	$C_n$	$C_y$
0.25	0.405	0.1035	-0.0245	-0.1136	-0.68	+0.42	0
4.4	0.614	0.1197	+0.0290	-0.1076	-0.72	0.30	0
8.5	0.806	0.1466	0.0780	-0.1022	-0.13	0.13	0
12.65	0.999	0.1936	0.1246	-0.0994	0	0	0
14.7	1.084	0.2210	0.1464	-0.0969	-0.17	0.38	0
16.75	1.171	0.2558	0.1681	-0.0952	-0.51	0.59	0
18.8	1.261	0.3219	0.2056	-0.0802	+0.17	+1.31	0
20.85	1.338	0.4148	0.2452	-0.0627	+0.38	-0.76	+3.38
22.9	1.425	0.5119	0.2830	-0.0500	-0.68	+0.13	-1.13
25.0	1.540	0.6194	+0.3254	-0.0398	+0.97	-0.30	-2.03
27.0	1.580						
29.0	1.584						
30.1	1.563						

TABLE 6

Model A. Comparison of Two Types of Trailing-Edge Flaps

$$\text{c.g. } \begin{cases} 0.52 \bar{c} & C_m \\ 0.30 \bar{c} & C_m' \end{cases} \quad \text{Model with nose flaps (2)}$$

No trailing-edge flaps.

Both ailerons 20 deg up

$\alpha$	$C_L$	$C_D$	$C_m$	$C_m'$
2.1	-0.038	0.0330	0.1261	0.1339
4.1	+0.069	0.0288	0.1510	0.1354
8.3	0.282	0.0336	0.1964	0.1341
9.35	0.328	0.0371	0.2047	0.1323
10.35	0.362	0.0400	0.2099	0.1302
11.4	0.418	0.0466	0.2203	0.1282
12.4	0.476	0.0589	0.2376	0.1326
13.45	0.518	0.0701	0.2489	0.1343
14.5	0.570	0.0864	0.2630	0.1365
16.55	0.661	0.1208	0.2847	0.1376
18.6	0.763	0.1707	0.3071	0.1356
20.65	0.849	0.2261	0.3356	0.1431
22.7	0.941	0.3060	0.3901	0.1729
24.8	+1.029	0.4138	0.4617	0.2179

Trailing-edge flaps (1).

Both ailerons 20 deg up

$\alpha$	$C_L$	$C_D$	$C_m$
0.1	-0.054	0.1026	0.1067
2.15	+0.012	0.0985	0.1268
4.2	0.104	0.0959	0.1525
8.3	0.269	0.0977	0.1974
9.35	0.326	0.1014	0.2103
10.35	0.362	0.1038	0.2179
11.4	0.410	0.1086	0.2282
12.4	0.441	0.1136	0.2359
13.45	0.485	0.1249	0.2503
14.45	0.530	0.1378	0.2116
16.5	0.586	0.1622	0.2851
18.55	0.662	0.2073	0.3147
20.6	0.740	0.2617	0.3511
22.65	0.799	0.3152	0.3907
24.65	+0.865	0.3943	0.4425

Trailing-edge flaps (2).

Both ailerons 20 deg up

$\alpha$	$C_L$	$C_D$	$C_m$
0.3	0.305	0.1383	0.0954
2.4	0.405	0.1396	0.1195
4.45	0.497	0.1442	0.1418
8.55	0.703	0.1662	0.1864
9.6	0.747	0.1711	0.1955
10.65	0.802	0.1751	0.2054
11.70	0.839	0.1835	0.2126
12.7	0.895	0.1972	0.2252
13.7	0.936	0.2111	0.2332
14.75	0.992	0.2298	0.2447
16.8	1.073	0.2745	0.2651
18.9	1.188	0.3583	0.2984
20.95	1.273	0.4516	0.3419
23.0	1.361	0.5500	0.3929
25.0	1.393	0.6279	0.4343

Trailing-edge flaps (2).

Both ailerons 10 deg up

$\alpha$	$C_L$	$C_D$	$C_m$
-3.7	0.318	0.1042	-0.1005
+0.45	0.528	0.1139	-0.0553
4.6	0.727	0.1386	-0.0044
8.7	0.909	0.1805	+0.0456
10.75	0.992	0.2038	0.0755
12.8	1.083	0.2364	0.1033
14.85	1.162	0.2710	0.1284
+16.9	1.255	0.3296	+0.1511

TABLE 7  
*Model A. Model with Tail*

$$\text{c.g. } \begin{cases} 0.52 \bar{c} \\ 0.30 \bar{c} \end{cases} \quad \begin{matrix} C_m \\ C_{m'} \end{matrix}$$

No flaps.  $\eta_T = 0$  deg

$\alpha$	$C_L$	$C_D$	$C_m$	$C_{m'}$
-0.95	-0.097	0.0133	0.0269	+0.0484
+0.1	-0.041	0.0126	0.0274	+0.0366
4.25	+0.194	0.0180	0.0272	-0.0159
6.35	0.321	0.0249	0.0262	-0.0444
8.4	0.424	0.0357	0.0262	-0.0668
10.45	0.553	0.0519	0.0269	-0.0950
12.55	0.648	0.1328	0.0567	-0.0886
16.65	0.867	0.2154	0.1178	-0.0784
20.8	1.058	0.3569	0.1976	-0.0481
24.85	1.162	0.4900	0.2935	+0.0162
+26.9	+1.196	0.5874	0.1182	-0.1742

No flaps.  $\eta_T = + 5$  deg

$\alpha$	$C_L$	$C_D$	$C_m$
0.11	-0.009	0.0130	-0.0301
4.28	0.253	0.0228	-0.0327
8.42	0.474	0.0433	-0.0341
12.57	0.708	0.1228	+0.0130
16.72	0.931	0.2394	0.0609
20.82	1.101	0.3683	0.1334
24.90	1.211	0.5072	0.2314
26.91	1.242	0.5750	+0.2804

Nose flaps (1).  $\eta_T = + 5$  deg

$\alpha$	$C_L$	$C_D$	$C_m$
0.05	0.048	0.0216	-0.0460
4.15	0.259	0.0252	-0.0406
8.3	0.483	0.0422	-0.0235
10.4	0.592	0.0649	-0.0304
12.45	0.700	0.1090	+0.0025
14.5	0.817	0.1606	0.0133
16.6	0.930	0.2208	0.0396
18.65	1.045	0.2905	0.0680
20.7	1.131	0.2512	0.0954
22.75	1.205	0.4133	0.1299
24.8	1.253	0.4785	+0.1583

Nose flaps (2) (without Plasticine).  
 $\eta_T = + 5$  deg

$\alpha$	$C_L$	$C_D$	$C_m$
0.15	0.025	0.0270	-0.0432
4.3	0.266	0.0283	-0.0290
8.45	0.516	0.0505	-0.0182
9.5	0.569	0.0577	-0.0161
10.5	0.630	0.0702	-0.0143
11.55	0.686	0.0843	-0.0106
12.6	0.742	0.1064	+0.0003
14.65	0.830	0.1450	0.0163
16.7	0.934	0.1525	0.0422
18.8	1.066	0.2409	0.0847
20.85	1.148	0.3432	0.1257
24.95	1.283	0.4919	0.2128
27.0	1.334	0.5797	+0.2874

Nose flaps (1) and (2).  $\eta_T = + 5$  deg

$\alpha$	$C_L$	$C_D$	$C_m$
0	0.012	0.0342	-0.0645
2.1	0.129	0.0303	-0.0534
4.15	0.254	0.0310	-0.0436
6.25	0.377	0.0363	-0.0348
8.3	0.490	0.0452	-0.0259
9.35	0.554	0.0532	-0.0222
10.3	0.597	0.0603	-0.0199

$\alpha$	$C_L$	$C_D$	$C_m$
12.45	0.715	0.0841	-0.0132
14.55	0.828	0.1140	-0.0082
16.6	0.932	0.1506	+0.0025
18.65	1.032	0.1991	0.0170
20.75	1.166	0.2807	0.0388
22.8	1.268	0.3656	+0.0838
24.85	1.355	0.4543	

TABLE 7—*continued*Trailing-edge flaps (2).  $\eta_T = +5$  deg

$\alpha$	$C_L$	$C_D$	$C_m$
0.4	0.464	0.1078	-0.0190
2.5	0.575	0.1162	-0.0182
4.55	0.694	0.1329	-0.0183
8.7	0.901	0.1761	-0.0121
9.75	0.964	0.2020	-0.0007
10.75	1.021	0.2287	+0.0109
11.8	1.083	0.2741	0.0453
12.8	1.099	0.2987	0.0582
13.9	1.179	0.3345	0.0730
14.9	1.225	0.3634	0.0849
16.95	1.318	0.4317	0.1134
19.0	1.411	0.5101	0.1459
21.05	1.499	0.5913	0.1817
23.15	1.572	0.6806	+0.2239

Trailing-edge flaps (2). Nose flaps (1).  
 $\eta_T = +5$  deg

$\alpha$	$C_L$	$C_D$	$C_m$
0.25	0.415	0.1021	-0.0284
4.4	0.631	0.1205	-0.0195
8.55	0.845	0.1598	-0.0068
10.6	0.948	0.2066	+0.0150
12.65	1.043	0.2534	0.0355
14.75	1.153	0.3141	0.0617
16.8	1.258	0.3844	0.1014
18.85	1.333	0.4530	0.1165
20.9	1.435	0.5357	0.1446
22.95	1.517	0.6154	0.1683
25.0	1.570	0.6930	+0.2213

Trailing-edge flaps (2). Nose flaps (2).  
 $\eta_T = +5$  deg

$\alpha$	$C_L$	$C_D$	$C_m$
-3.75	0.196	0.1113	-0.0363
+0.4	0.438	0.1141	-0.0192
2.45	0.541	0.1212	-0.0111
4.55	0.680	0.1335	-0.0034
8.7	0.907	0.1725	+0.0091
9.75	0.962	0.1841	0.0118
10.75	1.015	0.1515	0.0140
11.8	1.081	0.2172	0.0198
12.85	1.133	0.2365	0.0259
13.85	1.172	0.2533	0.0314
14.9	1.223	0.2778	0.0401
16.95	1.315	0.3381	0.0569
19.05	1.423	0.4259	0.0886
+21.05	1.491	0.5293	+0.1653

Trailing-edge flaps (2). Nose flaps (1) and (2).  
 $\eta_T = +5$  deg

$\alpha$	$C_L$	$C_D$	$C_m$
-3.9	0.137	0.1044	-0.0538
-1.85	0.251	0.1030	-0.0441
+0.25	0.378	0.1064	-0.0320
2.3	0.504	0.1136	-0.0197
4.4	0.615	0.1233	-0.0094
6.5	0.751	0.1412	+0.0026
8.55	0.855	0.1572	0.0092
10.6	0.949	0.1773	0.0153
12.7	1.069	0.2098	0.0221
14.75	1.166	0.2422	0.0283
16.8	1.260	0.2807	0.0355
18.9	1.369	0.3504	0.0549
20.95	1.455	0.4562	0.1224
+23.0	1.531	0.5502	+0.1598

TABLE 8

*Model A. Tests to Determine Downwash*

Model with Tail and Nose Flaps (2). Both Ailerons 20 deg up

$$\text{c.g. } \begin{cases} 0.52 \bar{\epsilon} \\ 0.42 \bar{\epsilon} \end{cases} \quad \begin{matrix} C_m \\ C_m' \end{matrix}$$

No trailing-edge flaps.  $\eta_T = + 5$  deg

$\alpha$	$C_L$	$C_D$	$C_m$	$C_m'$
0.05	-0.122	0.0454	0.0559	0.0682
2.1	-0.008	0.0389	0.0644	0.0650
4.2	+0.115	0.0363	0.0716	0.0599
8.35	0.369	0.0475	0.0796	0.0425
9.4	0.411	0.0523	0.0795	0.0380
10.45	0.481	0.0607	0.0788	0.0303
11.45	0.534	0.0692	0.0783	0.0256
12.5	0.594	0.0840	0.0881	0.0253
13.55	0.637	0.0981	0.0964	0.0290
14.55	0.693	0.1156	0.1045	0.0315
16.6	0.789	0.1574	0.1193	0.0361
18.7	0.899	0.2138	0.1389	0.0436
20.75	0.999	0.2839	0.1742	0.0685
22.8	1.088	0.3695	0.2347	0.1169
24.85	+1.152	0.4619	0.3129	0.1859

No trailing-edge flaps.  $\eta_T = - 5$  deg

$\alpha$	$C_L$	$C_D$	$C_m$
2.05	-0.118	0.0385	0.1728
4.0	+0.004	0.0324	0.1814
8.25	0.220	0.0346	0.1911
9.3	0.302	0.0383	0.1930
10.35	0.371	0.0441	0.1942
11.4	0.431	0.0510	0.1948
12.45	0.481	0.0604	0.1993
13.45	0.526	0.0709	0.2050
14.5	0.582	0.0867	0.2123
16.55	0.692	0.1268	0.2260
18.6	0.789	0.1720	0.2416
20.7	0.894	0.2390	0.2777
22.75	0.975	0.3147	0.3314
24.8	1.050	0.3990	0.4158
26.8	+1.073	0.4638	0.4802

Trailing-edge flaps (1).  $\eta_T = - 5$  deg

$\alpha$	$C_L$	$C_D$	$C_m$
4.15	0.036	0.1009	0.1902
8.3	0.247	0.1018	0.2013
9.3	0.303	0.1042	0.2025
10.35	0.350	0.1073	0.2030
11.4	0.408	0.1119	0.2030
12.4	0.452	0.1205	0.2054
13.45	0.497	0.1299	0.2122
14.45	0.543	0.1416	0.2194
16.5	0.623	0.1733	0.2327
20.6	0.775	0.2681	0.2842
22.65	0.834	0.3258	0.3295
24.7	0.891	0.4037	0.3730

Trailing-edge flaps (1).  $\eta_T = + 5$  deg

$\alpha$	$C_L$	$C_D$	$C_m$	$C_m'$
2.15	0.047	0.1054	0.0738	0.0686
4.2	0.157	0.1045	0.0804	0.0639
8.35	0.361	0.1122	0.0886	0.0511
9.4	0.402	0.1166	0.0895	0.0478
10.5	0.473	0.1235	0.0879	0.0392
11.45	0.518	0.1300	0.0873	0.0338
12.5	0.571	0.1410	0.0909	0.0322
13.5	0.625	0.1582	0.1013	0.0367
14.55	0.666	0.1739	0.1087	0.0400
16.6	0.736	0.2107	0.1257	0.0492
18.65	0.802	0.2522	0.1461	0.0619
20.7	0.876	0.3100	0.1794	0.0865
22.7	0.940	0.3789	0.2280	0.1268
24.75	1.001	0.4538	0.2943	0.1847

TABLE 8—*continued*Trailing-edge flaps (2).  $\eta_T = + 5$  deg

$\alpha$	$C_L$	$C_D$	$C_m$	$C_{m'}$
0·4	0·297	0·1414	0·0873	0·0575
2·4	0·403	0·1435	0·0950	0·0544
4·45	0·515	0·1494	0·1021	0·0496
8·6	0·742	0·1730	0·1114	0·0356
9·65	0·814	0·1822	0·1134	0·0301
10·65	0·861	0·1892	0·1137	0·0256
11·7	0·922	0·2027	0·1164	0·0220
12·75	0·974	0·2154	0·1206	0·0208
13·8	1·028	0·2310	0·1232	0·0178
14·8	1·091	0·2550	0·1280	0·0159
16·85	1·178	0·3057	0·1414	0·0199
18·95	1·290	0·3888	0·1707	0·0357
21·0	1·375	0·4938	0·2260	0·0800
23·05	1·455	0·5914	0·2943	0·1374
25·05	1·487	0·6810	0·3570	0·1937

Trailing-edge flaps (2).  $\eta_T = - 5$  deg

$\alpha$	$C_L$	$C_D$	$C_m$
0·25	0·188	0·1441	0·1998
2·3	0·283	0·1423	0·2068
4·4	0·403	0·1449	0·2136
8·5	0·632	0·1613	0·2245
9·55	0·693	0·1669	0·2263
10·6	0·759	0·1738	0·2275
13·7	0·936	0·2140	0·2384
14·75	0·982	0·2298	0·2422
16·8	1·083	0·2838	0·2582
18·9	1·189	0·3604	0·2869
20·95	1·261	0·4445	0·3344
23·0	1·345	0·5489	0·4093
25·0	1·339	0·6198	0·4684

TABLE 9

Model A. Effect of Sideslip

No flaps.  $\beta = 0$  deg

$\alpha$	$C_L$	$C_t$	$C_n$	$C_y$
0	0.009	-1.08	+0.17	-4.50
4.15	0.199	-1.48	+0.08	-5.62
8.25	0.395	-1.86	-0.08	-6.30
10.3	0.489	-1.95	-0.04	-6.75
12.4	0.593	-2.54	-0.55	+0.90
14.45	0.707	-2.45	-0.25	-5.17
16.5	0.792	-2.79	-0.25	-4.50
18.55	0.879	-3.25	+0.13	-4.95
20.6	0.952	-4.35	+0.30	-4.95

No flaps.  $\beta = + 5$  deg

$\alpha$	$C_L$	$C_t$	$C_n$	$C_{y1}$	$C_y$
0	0.016	-0.66	-3.17	-4.05	-4.802
2.05	0.108	-2.73	-3.00	-1.80	
4.15	0.198	-5.56	-3.05	-1.13	-2.390
6.2	0.288	-7.72	-2.41	-2.25	-4.230
8.25	0.377	-10.08	-1.90	-4.50	-7.038
10.3	0.483	-13.49	-4.36	+11.00	+7.113
12.4	0.598	-14.64	-2.50	13.50	-4.5892
14.45	0.700	-14.44	-1.02	9.45	
16.5	0.786	-13.49	-0.47	12.15	-5.8594
18.55	0.870	-11.94	0	11.25	
20.6	0.959	-9.07	-0.38	13.05	-16.020
22.65	1.031	-7.21	-0.76	19.35	
24.7	1.084	-5.69	-0.59	+20.25	-20.942

No flaps.  $\beta = - 5$  deg

$\alpha$	$C_L$	$C_t$	$C_n$	$C_{y1}$	$C_y$
0	0.004	0.03	3.55	+ 1.35	- 2.1119
2.05	0.102	2.44	3.26	+ 1.35	
4.1	0.190	5.06	3.21	+ 0.45	- 1.713
6.2	0.287	7.55	2.66	0	1.988
8.25	0.381	9.79	1.86	0	- 2.555
9.3	0.438	11.73	3.93	-10.36	- 7.216
10.3	0.481	12.90	4.82	-16.66	- 12.751
11.35	0.527	12.88	4.44	-18.02	- 12.048
12.35	0.583	12.79	3.43	-20.94	- 12.001
14.45	0.682	11.78	1.02	-10.13	
16.5	0.780	11.39	0.59	-8.33	+ 9.665
18.55	0.865	9.50	0.64	-14.86	
20.6	0.963	5.19	1.27	-15.76	+13.320
22.65	1.034	3.83	1.57	-20.04	
24.7	1.083	3.03	1.44	-21.84	+19.358

TABLE 9—*continued*Nose flaps (1) and (2).  $\beta = 0$  deg

$\alpha$	$C_L$	$C_D$	$C_m$	$C_t$	$C_n$	$C_y$
0	-0.018	0.0292	-0.0229	+0.42	+0.13	+7.88
4.1	+0.186	0.0225	+0.0312	-0.63	0	1.80
8.25	0.388	0.0317	0.0830	-0.47	-0.21	0
12.35	0.584	0.0576	0.1321	-0.34	-0.09	1.13
14.45	0.692	0.0820	0.1529	-0.13	-0.13	1.13
16.5	0.775	0.1069	0.1720	-0.04	-0.13	+0.45
18.55	0.874	0.1468	0.1978	0	+0.47	-1.13
20.65	0.997	0.2157	0.2205	+1.10	+0.97	-5.63
22.7	+1.104	0.3023	+0.2708	+0.42	-0.30	-1.58

Nose flaps (1) and (2).  $\beta = + 5$  deg

$\alpha$	$C_L$	$C_D$	$C_m$	$C_t$	$C_n$	$C_y$
0	-0.003	0.0290	-0.0214	-0.83	-3.17	-11.727
4.15	+0.202	0.0227	+0.0337	-6.16	-3.25	-9.383
8.25	0.398	0.0315	0.0848	-11.57	-2.15	-8.355
12.35	0.596	0.0584	0.1334	-15.62	-1.31	-9.131
14.45	0.699	0.0815	0.1547	-17.94	-0.63	-4.865
16.5	0.791	0.1107	0.1764	-21.03	-0.04	-5.390
19.0	0.920	0.1653	0.2037	-20.18	+0.38	+9.815
20.65	0.999	0.2109	0.2319	-22.42	-5.32	24.683
22.7	+1.105	0.2881	+0.2740	-19.80	-5.11	19.747

Nose flaps (1) and (2).  $\beta = - 5$  deg

$\alpha$	$C_L$	$C_D$	$C_m$	$C_t$	$C_n$	$C_y$
0	0	0.0291	-0.0202	-0.52	3.29	+ 7.698
4.1	0.192	0.0233	+0.0308	+ 4.76	3.00	6.294
8.25	0.386	0.0317	0.0807	10.59	1.86	6.129
12.35	0.580	0.0674	0.1296	15.07	0.97	8.345
14.45	0.676	0.0782	0.1503	16.97	0.67	6.206
16.5	0.784	0.1109	0.1749	20.65	0.34	+ 2.043
18.55	0.881	0.1502	0.1942	20.78	3.67	-10.235
20.6	0.971	0.1987	0.2281	22.17	6.04	-28.888
22.7	1.093	0.2795	+0.2686	+20.82	3.50	-32.162

TABLE 9—*continued*Trailing-edge flaps (2). Nose flaps (1) and (2).  $\beta = 0$  deg

$\alpha$	$C_L$	$C_D$	$C_m$	$C_i$	$C_n$	$C_y$
0·25	0·405	0·1035	-0·0245	-0·68	+0·42	0
4·4	0·614	0·1197	+0·0290	-0·72	0·30	0
8·5	0·806	0·1466	0·0780	-0·13	0·13	0
12·65	0·999	0·1936	0·1246	0	0	0
14·7	1·084	0·2210	0·1464	-0·17	0·38	0
16·75	1·171	0·2558	0·1681	-0·51	0·59	0
18·8	1·261	0·3219	0·2056	+0·17	+1·31	0
20·85	1·338	0·4148	0·2452	+0·38	-0·76	+3·38
22·9	1·425	0·5119	+0·2830	-0·68	+0·13	-1·13

Trailing-edge flaps (2). Nose flaps (1) and (2).  $\beta = +5$  deg

$\alpha$	$C_L$	$C_D$	$C_m$	$C_i$	$C_n$	$C_y$
0·25	0·396	0·1009	-0·0194	-7·17	-2·53	-7·677
4·4	0·601	0·1174	+0·0314	-13·21	-0·97	-10·911
8·5	0·769	0·1461	0·0806	-18·28	+1·65	-12·740
12·65	0·979	0·1912	0·1252	-22·34	4·69	-16·673
14·7	1·074	0·2227	0·1500	-24·92	5·79	-15·606
16·75	1·168	0·2641	0·1811	-22·21	+1·57	-2·839
18·8	1·259	0·3198	0·2046	-26·56	-3·97	+26·180
20·85	1·322	0·3978	0·2500	-16·59	-0·55	+15·565
22·9	1·408	0·4964	+0·2903	-8·99	+0·55	+0·909

Trailing-edge flaps. Nose flaps (1) and (2).  $\beta = -5$  deg

$\alpha$	$C_L$	$C_D$	$C_m$	$C_i$	$C_n$	$C_y$
0·25	0·396	0·1061	-0·0223	6·58	+3·04	+9·925
4·4	0·600	0·1225	+0·0301	13·04	+1·05	13·599
8·5	0·798	0·1525	0·0787	17·86	-1·40	14·868
12·6	0·973	0·1953	0·1222	23·14	-4·52	19·498
14·7	1·063	0·2241	0·1469	24·96	-5·62	17·074
16·75	1·164	0·2681	0·1687	22·63	-0·85	+2·514
18·8	1·254	0·3232	0·2050	25·72	+4·35	-25·660
20·85	1·321	0·4058	0·2514	16·04	+1·35	-18·681
22·9	1·403	0·4943	+0·2888	10·80	-1·40	-2·663

TABLE 9—*continued*

Traverse of Angles of Sideslip

No flaps.  $\alpha = 16 \cdot 6$  deg

$\beta$	$C_t$	$C_n$
+5.0	-14.64	-0.76
2.5	-8.11	-0.55
+1.25	-0.42	-0.34
0	-0.97	-0.17
-1.25	+2.69	+0.17
-2.5	+5.95	+0.38
-5.0	+12.12	

Nose flaps (1) and (2).  $\alpha = 16 \cdot 6$  deg

$\beta$	$C_L$	$C_D$	$C_m$	$C_t$	$C_n$	$C_y$
+15.0	0.777	0.1229	0.1901	-52.27	-4.30	+2.126
10.0	0.799	0.1202	0.1795	-36.41	-4.09	+1.742
5.0	0.795	0.1121	0.1782	-20.09	-0.43	-4.167
+2.5	0.1117				0	-2.622
0	0.800	0.1110	0.1798	+1.06	-0.35	-0.45
-2.5	0.1107				-0.25	+4.827
-5.0	0.792	0.1123	0.1792	22.04	+0.76	-2.321
-10.0	0.785	0.1197	0.1800	37.61	+4.13	-9.146
-15.0	0.762	0.1208	0.1917	+53.27	+4.22	-8.329

Trailing-edge flaps (2). Nose flaps (1) and (2).  $\alpha = 16 \cdot 6$  deg

$\beta$	$C_L$	$C_D$	$C_m$	$C_t$	$C_n$	$C_y$
+10.0	1.152	0.2716	0.1819	-49.51	+2.71	+5.382
5.0	1.155	0.2592	0.1671	-24.04	2.45	-3.535
2.5	1.148	0.2510	0.1687	-13.77	2.58	-3.970
+1.25	1.153	0.2508	0.1666	-7.18	+1.52	-3.666
0	1.160	0.2522	0.1649	0	0	0
-1.25	1.157	0.2603	0.1693	+7.10	-1.94	+2.522
-2.5	1.158	0.2687	0.1709	11.70	-2.41	+4.965
-5.0	1.159	0.2611	0.1681	22.44	-1.56	+1.459
-10.0	1.148	0.2500	0.1815	51.51	-2.59	-12.019
-15.0	1.130	0.2508	0.1946	+79.97	-4.10	-41.458

TABLE 10

*Model A. Effect of Aileron Deflection*

Ailerons—flap type

Nose flaps (1) and (2).  $\xi = \begin{cases} 20 \text{ deg up port} \\ 10 \text{ deg down starboard.} \end{cases}$   $\alpha = 16.6 \text{ deg}$

$\beta$	$C_l$	$C_n$	$C_y$
+15.0	-78.67	3.56	+37.16
10.0	-69.11	4.95	26.35
5.0	-54.84	8.12	13.96
2.5	-45.87	8.33	11.26
+ 1.25	-40.84	8.02	11.03
0	-36.17	7.73	9.46
- 1.25	-29.46	7.44	7.66
- 2.5	-23.83	7.39	7.21
- 5.0	-14.26	7.60	+ 3.60
-10.0	+ 0.55	10.34	-10.81
-12.5	+ 9.64	11.42	-19.37
-15.0	+18.07	11.53	-23.65

Nose flaps (1) and (2). Trailing-edge flaps (2).  $\xi = \begin{cases} 20 \text{ deg up port} \\ 10 \text{ deg down starboard.} \end{cases}$   $\alpha = 16.6 \text{ deg}$

$\beta$	$C_l$	$C_n$	$C_y$
+15.0	-101.37	10.50	+87.15
10.0	- 77.11	8.42	59.23
5.0	- 53.34	8.58	25.45
2.5	- 24.17	9.19	11.94
+ 1.25	- 35.24	8.61	6.98
0	- 29.19	7.52	4.05
- 1.25	- 23.16	6.17	+ 1.58
- 2.5	- 18.63	6.08	- 3.38
- 5.0	- 6.66	6.20	-16.44
-10.0	+ 23.71	4.62	-49.99
-15.0	+ 50.97	2.87	-80.17

TABLE 10—*continued*  
 Ailerons—flap type. Port aileron only moved  
 $\xi = + 10$  deg port. No flaps

$\alpha$	$C_L$	$C_D$	$C_m$	$C_i$	$C_n$	$C_y$
0	-0.023	0.0140	0.0338	-14.28	-0.37	0.45
4.1	+0.161	0.0142	0.0669	-14.28	-0.30	3.15
8.25	0.352	0.0234	0.0981	-13.14	+0.04	6.08
10.3	0.455	0.0425	0.1206	-12.38	1.27	4.05
11.3	0.498	0.0583	0.1316	-12.55	1.61	2.70
12.35	0.572	0.0884	0.1558	-12.96	0.80	13.51
13.4	0.603	0.1174	0.1777	-13.10	1.40	9.46
14.45	0.673	0.1339	0.1896	-12.29	1.82	6.98
16.5	0.770	0.1869	0.2223	-11.86	2.45	5.86
18.55	0.868	0.2421	0.2559	-12.16	3.29	5.63
20.6	+0.945	0.3065	0.2975	-12.84	+4.23	4.95

$\xi = + 20$  deg port. No flaps

$\alpha$	$C_L$	$C_D$	$C_m$	$C_i$	$C_n$	$C_y$
-0.05	-0.067	0.0231	0.0627	-27.89	-3.68	-1.35
+4.1	+0.126	0.0183	0.0921	-28.60	-1.90	+0.90
8.2	0.311	0.0261	0.1223	-26.90	-1.10	4.95
10.25	0.406	0.0371	0.1377	-25.55	-0.34	6.08
10.8	0.436	0.0476	0.1456	-24.50	+1.99	0.68
11.3	0.462	0.0605	0.1545	-24.60	1.06	0.68
11.8	0.484	0.0687	0.1611	-24.54	1.14	6.31
12.35	0.523	0.0876	0.1756	-24.73	0.76	13.96
12.85	0.548	0.0975	0.1817	-24.43	1.10	14.41
13.4	0.591	0.1167	0.1964	-23.64	1.99	8.11
14.4	0.636	0.1366	0.2109	-23.19	2.34	8.56
16.45	0.733	0.1835	0.2403	-21.96	3.42	7.43
18.55	0.828	0.2389	0.2739	-21.50	4.94	5.86
+20.6	+0.912	0.2983	0.3095	-21.76	+6.22	+6.08

TABLE 10—*continued*

Ailerons—flap type

 $\xi = -10$  deg port. No flaps

$\alpha$	$C_L$	$C_D$	$C_m$	$C_t$	$C_n$	$C_y$
0.05	0.056	0.0153	-0.0263	13.98	-0.30	+2.70
4.15	0.243	0.0193	+0.0075	13.39	-1.61	0.90
6.2	0.339	0.0273	0.0269	12.89	-1.90	2.25
8.3	0.438	0.0374	0.0455	12.00	-3.13	3.15
9.3	0.478	0.0437	0.0528	12.00	-3.74	+1.80
10.35	0.533	0.0588	0.0648	12.41	-2.47	-3.60
10.85	0.550	0.0644	0.0715	12.12	-2.58	-3.38
11.35	0.578	0.0777	0.0803	12.08	-2.79	-1.13
11.9	0.609	0.0918	0.0914	11.65	-3.42	+3.15
12.4	0.639	0.1074	0.1052	10.39	-3.83	13.51
12.95	0.678	0.1272	0.1210	10.18	-3.42	4.95
13.45	0.690	0.1334	0.1253	10.55	-3.29	2.25
14.45	0.737	0.1573	0.1429	10.65	-3.46	1.80
16.55	0.824	0.2049	0.1735	9.42	-3.59	1.35
18.6	0.924	0.2702	+0.2125	9.00	-3.80	+0.23

 $\xi = +10$  deg port. Nose flaps (1) and (2)

$\alpha$	$C_L$	$C_D$	$C_m$	$C_t$	$C_n$	$C_y$
0.05	0.041	0.0309	0.0058	-13.60	-0.38	1.13
4.1	0.159	0.0225	0.0599	-13.60	-0.21	2.25
8.25	0.354	0.0281	0.1092	-12.67	+0.04	4.50
12.35	0.558	0.0514	0.1578	-11.65	1.10	2.70
14.4	0.659	0.0724	0.1780	-11.62	1.82	3.38
16.5	0.758	0.1002	0.2009	-10.90	2.32	2.25
18.55	0.852	0.1380	0.2224	-10.94	+3.13	1.35

TABLE 10—*continued*

## Ailerons—flap type

 $\xi = + 20$  deg port. Nose flaps (1) and (2)

$\alpha$	$C_L$	$C_D$	$C_m$	$C_t$	$C_n$	$C_y$
- 0.05	-0.074	0.0394	0.0376	-27.61	-3.25	3.60
+ 4.05	+0.101	0.0283	0.0723	-27.91	-2.03	5.40
8.2	0.300	0.0301	0.1258	-27.32	-1.04	7.66
10.25	0.419			-26.49	-0.42	9.46
12.3	0.500	0.0487	0.1802	-25.05	+0.25	9.68
14.4	0.605	0.0677	0.2001	-24.62	1.48	10.13
16.45	0.705	0.0927	0.2222	-24.31	2.96	9.91
18.5	0.803	0.1277	0.2458	-23.20	4.35	8.78
20.6	0.927			-23.45	6.71	3.60
22.65	1.017			-21.08	6.55	4.50
+24.7	+1.105			-22.36	+7.43	0.45

 $\xi = - 10$  deg port. Nose flaps (1) and (2)

$\alpha$	$C_L$	$C_D$	$C_m$	$C_t$	$C_n$	$C_y$
0.05	0.049	0.0295	-0.0421	12.96	-0.26	+0.68
4.15	0.253	0.0276	+0.0119	13.35	-1.31	-0.45
8.3	0.441	0.0408	0.0625	12.71	-3.21	+0.68
10.35	0.540	0.0529	0.0665	12.16	-4.27	+7.88
12.4	0.629	0.0695	0.1112	11.11	-5.45	-3.60
14.45	0.728	0.0927	0.1292	11.56	-5.87	+4.05
16.55	0.827	0.1225	0.1530	11.82	-5.74	+2.03
17.5	0.863	0.1364	0.1656	10.90	-5.20	+2.25
18.6	0.914	0.1581	0.1784	10.90	-4.56	-0.90
19.6	0.978	0.1908	0.1876	10.52	-3.55	-3.15
20.65	1.054	0.2360	0.2016	13.69	-4.44	-6.76
21.75	1.091	0.2694	0.2271	11.19	-4.61	-3.60
22.65	1.161	0.3286	0.2573	11.62	-6.04	-2.70
24.8	1.232	0.4070	+0.3089	10.98	-6.59	-6.31

TABLE 10—*continued*

No flaps

Ailerons—delta type

 $\xi = 0$  deg

$\alpha$	$C_L$	$C_D$	$C_m$	$C_t$	$C_n$	$C_y$
0	0.018	0.0117	0.0022	-0.21	-0.13	+0.45
4.15	0.204	0.0141	0.0370	-0.59	-0.08	+0.68
8.25	0.384	0.0252	0.0721	-0.63	-0.13	0
10.3	0.489	0.0448	0.0924	+0.38	+1.23	-4.95
12.4	0.601	0.0953	0.1305	-0.89	-0.76	+7.66
14.45	0.705	0.1470	0.1669	-1.35	+0.04	2.03
16.5	0.797	0.1968	0.1976	-1.86	0.30	2.03
18.55	0.884	0.2503	0.2292	-2.32	0.59	2.70
20.6	0.975	0.3176	0.2695	-2.07	0.80	2.03
22.65	1.049	0.3862	0.3116	-1.65	0.59	3.15
24.7	1.108	0.4585		-1.69	+0.80	+3.38

 $\xi = +10$  deg port

$\alpha$	$C_L$	$C_D$	$C_m$	$C_t$	$C_n$	$C_y$
0	-0.016	0.0131	0.0160	-9.34	-0.04	-3.15
4.1	+0.176	0.0139	0.0508	-9.20	-0.38	0
8.25	0.360	0.0232	0.0852	-9.50	-0.89	+2.25
10.3	0.461	0.0409	0.1044	-8.54	+0.42	-2.03
11.35	0.517	0.0626	0.1234	-8.96	0.89	+0.90
12.35	0.567	0.0859	0.1389	-8.24	0.59	6.76
14.45	0.675	0.1378	0.1798	-9.16	2.66	-0.68
16.45	0.740	0.1827	0.2089	-9.31	3.93	-3.15
18.55	0.856	0.2410	0.2461	-10.06	5.80	-4.95
20.6	0.940	0.3045	0.2859	-10.90	7.31	-5.86
22.65	+1.006	0.3708	0.3257	-10.65	+8.83	-6.53

TABLE 10—*continued*

Ailerons—delta type

 $\xi = + 20$  deg port

$\alpha$	$C_L$	$C_D$	$C_m$	$C_t$	$C_n$	$C_y$
0	-0.037	0.0214	0.0325	-19.05	-2.91	-3.60
4.1	+0.149	0.0188	0.0660	-19.10	-1.48	-0.68
8.2	0.337	0.0276	0.0987	-18.75	-2.07	+6.08
10.3	0.448	0.0454	0.1189	-16.70	-0.30	2.70
12.35	0.555	0.0884	0.1515	-15.75	0	13.51
14.45	0.666	0.1389	0.1903	-15.86	+2.19	5.40
16.5	0.756	0.1843	0.2196	-15.86	3.63	4.05
18.55	0.851	0.2436	0.2589	-16.05	5.80	3.38
20.6	0.932	0.3043	0.2942	-16.60	7.40	2.03
22.65	+0.988	0.3616	0.3323	-18.10	+8.96	+2.25

 $\xi = - 10$  deg port

$\alpha$	$C_L$	$C_D$	$C_m$	$C_t$	$C_n$	$C_y$
0	0.038	0.0126	-0.0111	8.45	-0.17	-3.83
4.15	0.226	0.0177	+0.0236	8.53	-0.46	-4.95
8.25	0.412	0.0354	0.0567	8.45	-4.01	-1.80
10.3	0.507	0.0551	0.0760	8.58	-3.85	-6.31
12.4	0.614	0.1021	0.1144	7.26	-2.92	0
14.45	0.714	0.1533	0.1514	5.78	-1.73	-8.56
16.5	0.808	0.2064	0.1857	4.05	-1.23	-8.56
18.55	0.895	0.2626	0.2211	3.17	-0.59	-9.01
20.6	0.972	0.3236	0.2565	2.24	-0.38	-9.91
22.65	1.038	0.3859	+0.2923	2.66	-1.06	-7.43

TABLE 11  
*Model B. Effect of Nose Flaps and Trailing-Edge Flaps*  
c.g.  $0.280\bar{c}$

No flaps

$\alpha$	$C_L$	$C_D$	$C_m$	$C_t$	$C_n$	$C_y$
0	0.007	0.0101	+0.0003	+0.21	-0.06	+0.35
4.15	0.198	0.0129	-0.0026	+0.06	-0.26	0
8.35	0.398	0.0259	-0.0069	-0.38	-0.44	0.70
10.4	0.490	0.0380	-0.0097	-0.62	-0.56	0.70
12.5	0.602	0.0700	-0.0171	-3.84	+0.97	1.76
14.6	0.732	0.1398	-0.0184	-1.58	0.68	+3.52
16.7	0.826	0.1971	-0.0008	-2.05	+1.26	-3.52
18.8	0.919	0.2651	+0.0259			
20.85	0.984	0.3236	0.0411			
22.85	1.025	0.3711	0.0558			
24.95	1.104	0.4546	+0.0695			

Nose flaps (3)

Nose flaps (2) and (3)

$\alpha$	$C_L$	$C_D$	$C_m$	$\alpha$	$C_L$	$C_D$	$C_m$
0	-0.004	0.0199	-0.0049	0	-0.008	0.0267	-0.0127
4.15	+0.195	0.0182	-0.0051	4.15	+0.195	0.0213	-0.0057
8.35	0.395	0.0287	-0.0077	8.35	0.402	0.0303	-0.0044
10.4	0.497	0.0406	-0.0091	10.45	0.503	0.0408	-0.0037
12.5	0.590	0.0603	-0.0102	12.5	0.605	0.0570	-0.0041
14.6	0.687	0.1026	-0.0042	14.6	0.711	0.0826	-0.0122
16.65	0.768	0.1529	+0.0096	16.7	0.829	0.1370	-0.0147
18.7	0.845	0.2074	0.0212	18.8	0.929	0.1962	-0.0034
20.8	0.923	0.2624	0.0344	20.85	1.019	0.2599	+0.0162
22.85	0.990	0.3213	0.0384	22.95	1.105	0.3432	+0.0453
24.9	1.059	0.3862	+0.0426	24.95	+1.138	0.4022	+0.0721
26.95	+1.107						

TABLE 11—*continued*

Nose flaps (1), (2) and (3)

$\alpha$	$C_L$	$C_D$	$C_m$
0	-0.012	0.0312	-0.0192
4.15	+0.191	0.0232	-0.0083
8.35	0.394	0.0304	-0.0033
10.45	0.503	0.0416	-0.0008
12.5	0.601	0.0576	+0.0004
14.6	0.708	0.0818	-0.0075
16.7	0.846	0.1263	-0.0233
18.8	0.972	0.1826	-0.0338
20.85	1.016	0.2288	+0.0053
22.9	1.065	0.2925	+0.0325
24.95	+1.128	0.3580	+0.0475

Trailing-edge flaps only

$\alpha$	$C_L$	$C_D$	$C_m$
0.4	0.468	0.1175	-0.1110
4.55	0.655	0.1370	-0.1194
9.05	0.859	0.1873	-0.1327
10.8	0.924	0.2243	-0.1280
12.85	1.008	0.3433	-0.1067
14.9	1.065	0.3977	-0.0848
16.95	1.103	0.4597	-0.0673

Trailing-edge flaps and nose flaps (1), (2) and (3)

$\alpha$	$C_L$	$C_D$	$C_m$	$C_i$	$C_n$	$C_y$
0.4	0.443	0.1206	-0.1067	-0.76	+0.03	-0.70
4.35	0.640	0.1356	-0.1051	-0.88	-0.03	-1.06
8.5	0.843	0.1658	-0.1107	-1.20	-0.26	0
10.6	0.941	0.1881	-0.1136	-1.47	-0.09	+0.18
12.7	1.038	0.2184	-0.1152	-1.00	+0.62	-2.47
14.8	1.174	0.3006	-0.1215	-2.58	3.49	-8.10
16.85	1.256	0.3725	-0.0995	-1.14	1.82	-5.64
18.9	1.293	0.4446	-0.0721	-3.29	2.05	-5.28
20.85	1.268	0.5030	-0.0520	-5.28	1.00	+1.41
22.9	1.294	0.5722	-0.0427	-8.16	2.76	0
25.2	1.326	0.6583	-0.0397	-6.60	3.20	0
27.15	1.343			-4.02	2.44	-0.35
29.15	1.345			-2.47	1.91	-1.41
30.15	1.345			-2.79	+2.08	-3.35

TABLE 11—*continued*  
Trailing-edge flaps and nose flaps (2) and (3)

$\alpha$	$C_L$	$C_D$	$C_m$	$C_i$	$C_n$
0.35	0.440	0.1215	-0.1090	-1.35	-0.23
4.55	0.656	0.1344	-0.1098	-1.47	-0.38
8.75	0.856	0.1627	-0.1168	-1.85	-0.41
10.8	0.951	0.1821	-0.1196	-2.11	-0.21
12.9	1.057	0.2122	-0.1215	-2.64	+0.18
15.0	1.156	0.2866	-0.1154	-3.08	+0.82
17.1	1.300	0.3826	-0.1063	-2.20	-0.15
19.15	1.370		-0.0819	-3.52	-0.53
21.15	1.343		-0.0428	-5.61	+0.12

Trailing-edge flaps and nose flaps (1)

$\alpha$	$C_L$	$C_D$	$C_m$	$C_i$	$C_n$	$C_y$
0.4	0.456	0.1166	-0.1089	-0.79	+0.03	-1.41
4.55	0.638	0.1326	-0.1124	-0.88	-0.38	0
8.7	0.845	0.1750	-0.1274	-0.88	-8.01	+0.88
10.8	0.953	0.2380	-0.1275	-4.29	-0.97	5.81
12.85	1.013	0.3332	-0.0942	-2.96	-1.26	8.10
14.9	1.069	0.3934	-0.0896	-2.64	+0.09	+1.41
16.95	1.116	0.4486	-0.0748	-1.41	+0.21	-0.70
18.95	1.149	0.5016	-0.0667	-1.91	+0.23	0
21.0	1.182	0.5663	-0.0593	-1.91	+0.21	-1.06
23.0	1.206	0.6234	-0.0529			
25.05	1.211	0.6842	-0.0488			

Trailing-edge flaps and nose flaps (3)

$\alpha$	$C_L$	$C_D$	$C_m$
0.4	0.467	0.1213	-0.1103
4.55	0.657	0.1379	-0.1158
8.7	0.852	0.1724	-0.1239
10.8	0.945	0.2058	-0.1248
12.9	1.038	0.2568	-0.1201
14.95	1.125	0.3294	-0.1117
17.0	1.184		-0.0961
19.05	1.245	0.4842	-0.0695
21.05	1.266	0.5506	-0.0562

TABLE 12  
*Model B. Effect of Sideslip*  
 Wing and fuselage alone  
 $\beta = + 5 \text{ deg}$

$\alpha$	$C_L$	$C_D$	$C_m$	$C_i$	$C_n$	$C_y$
0	0.008	0.0101	+0.0006	- 0.24	-2.30	- 2.285
4.15	0.201	0.0131	-0.0029	- 6.76	-2.09	- 2.726
8.35	0.388	0.0259	-0.0072	-12.48	-1.36	- 2.956
10.4	0.489	0.0395	-0.0115	-14.24	-2.06	+ 1.118
11.45	0.538	0.0526	-0.0137	-16.26	-4.88	+ 9.798
12.5	0.601	0.0728	-0.0175	-15.85	-7.90	+19.971
13.6	0.680	0.1052	-0.0369	-12.84	-4.70	+12.584
14.6	0.721	0.1273	-0.0260	-12.42	-3.00	+11.882
16.7	0.814	0.1910	-0.0017	- 7.61	-0.15	+ 0.888

$\beta = - 5 \text{ deg}$

$\alpha$	$C_L$	$C_D$	$C_m$	$C_i$	$C_n$	$C_y$
0	0.008	0.0099	0.0006	0.78	2.23	+ 2.965
4.15	0.198	0.0135	-0.0031	6.50	1.65	2.233
8.35	0.388	0.0260	-0.0081	11.66	0.54	3.323
10.4	0.483	0.0379	-0.0132	11.90	0.80	+ 2.428
12.5	0.613	0.0751	-0.0272	9.78	8.63	-14.152
13.55	0.660	0.0987	-0.0240	3.94	7.93	- 9.644
14.6	0.715	0.1288	-0.0198	0.92	7.17	-10.177
16.7	0.813	0.1895	-0.0015	4.35	3.00	- 3.828

TABLE 12—*continued*

Wing and fuselage with trailing-edge flaps and nose flaps (1), (2) and (3)

$$\beta = -5 \text{ deg}$$

$\alpha$	$C_L$	$C_D$	$C_m$	$C_i$	$C_n$	$C_y$
0·4	0·443	0·1233	-0·1071	10·14	2·65	+ 3·739
4·55	0·643	0·1397	-0·1065	16·09	2·65	+ 1·483
8·75	0·879	0·1907	-0·1216	18·18	6·58	- 9·691
10·6	0·966	0·2109	-0·1230	19·82	6·70	-13·189
12·6	1·061	0·2372	-0·1250	21·52	8·34	-19·672
14·35	1·138	0·2660	-0·1240	22·76	9·93	-25·579
17·05	1·243	0·3432	-0·1009	20·58	7·32	-20·949
19·7	1·293	0·4627	-0·0652	17·21	1·80	-13·338
21·4	1·301		-0·0478	7·41	2·65	

$$\beta = +5 \text{ deg}$$

$\alpha$	$C_L$	$C_D$	$C_m$	$C_i$	$C_n$	$C_y$
0·4	0·444	0·1238	-0·1078	-11·16	-2·44	- 4·828
4·55	0·646	0·1397	-0·1079	-17·24	-2·47	- 0·955
8·75	0·882	0·1919	-0·1209	-19·94	-6·82	+ 9·586
10·85	0·980	0·2133	-0·1224	-22·34	-6·58	11·047
12·9	1·071	0·2400	-0·1214	-24·40	-7·58	16·270
15·0	1·169	0·2851	-0·1107	-26·40	-7·40	18·305
17·05	1·237	0·3592	-0·0908	-22·17	-2·65	7·450
19·05	1·245	0·4368	-0·0696	-23·78	+0·43	+ 6·830
21·1	1·297		-0·1366	-14·86	+0·14	

TABLE 13  
*Model B. Effect of Aileron Deflection*  
 No flaps.  $\beta = 0$  deg  
 $\xi = + 10$  deg port

$\alpha$	$C_L$	$C_D$	$C_m$	$C_i$	$C_n$	$C_y$
0	-0.022	0.0111	+0.0248	-9.95	-0.59	0
4.05	+0.158	0.0120	0.0211	-9.92	-0.68	1.76
8.3	0.371	0.0238	0.0144	-9.51	-0.53	3.52
10.4	0.463	0.0345	0.0090	-8.57	-0.50	3.52
12.5	0.580	0.0677	-0.0018	-11.24	+1.03	5.28
14.6	0.706	0.1293	-0.0028	-8.86	2.67	3.87
16.7	0.806	0.1907	+0.0117	-7.10	3.17	-4.40

$\xi = + 20$  deg port

$\alpha$	$C_L$	$C_D$	$C_m$	$C_i$	$C_n$	$C_y$
-0.05	-0.048	0.0143	+0.0447	-18.29	-2.23	1.41
4.1	+0.143	0.0136	0.0401	-18.17	-2.11	4.58
8.3	0.340	0.0231	0.0324	-17.35	-1.67	6.69
10.4	0.448	0.0346	0.0229	-15.03	-1.41	5.64
12.45	0.555	0.0618	0.0101	-15.64	+1.20	9.16
14.6	0.692	0.1291	0.0080	-13.59	3.26	4.23
16.65	0.787	0.1839	0.0195	-11.33	4.11	-4.58

$\xi = - 10$  deg port

$\alpha$	$C_L$	$C_D$	$C_m$	$C_i$	$C_n$	$C_y$
0.05	0.032	0.0109	-0.0214	9.10	-0.56	0
4.2	0.222	0.0156	-0.0239	8.86	-0.97	-0.35
8.35	0.420	0.0303	-0.0274	7.60	-1.53	-1.41
10.45	0.513	0.0428	-0.0286	6.75	-1.70	-0.70
12.5	0.605	0.0717	-0.0327	1.48	-0.84	+2.11
14.65	0.740	0.1372	-0.0341	4.08	-1.38	4.58
16.7	0.846	0.2064	-0.0144	3.99	-1.41	3.70

TABLE 13—*continued*Nose flaps (1), (2) and (3) and trailing-edge flaps.  $\alpha = 12.7$  deg $\xi = 0$  deg

$\beta$	$C_L$	$C_D$	$C_m$	$C_i$	$C_n$	$C_y$
+5.0	1.072	0.2394	-0.1201	-24.69	-7.96	16.671
3.75	1.077	0.2440	-0.1222	-18.71	-7.63	16.384
2.5	1.068	0.2418	-0.1211	-12.34	-6.32	13.736
1.25	1.053	0.2278	-0.1155	-8.14	-1.95	4.362
0	1.056	0.2246	-0.1139	-1.41	+0.50	-1.76
-1.25	1.059	0.2293	-0.1144	+4.86	2.60	-6.099
-2.5	1.067	0.2413	-0.1208	9.02	6.99	-15.166
-3.75	1.071	0.2420	-0.1219	15.28	8.02	-17.743
-5.0	1.078	0.2435	-0.1233	20.85	8.75	-18.944

$$\xi = \begin{cases} \text{starboard 10 deg down} \\ \text{port 20 deg up} \end{cases}$$

$\beta$	$C_L$	$C_D$	$C_m$	$C_i$	$C_n$	$C_y$
+5.0	1.078	0.2467	-0.1181	-38.69	-7.46	23.406
3.75	1.077	0.2490	-0.1151	-31.45	-7.37	22.384
2.5	1.071	0.2524	-0.1119	-24.90	-6.91	21.546
1.25	1.074	0.2545	-0.1073	-19.21	-5.50	17.517
0	1.061	0.2531	-0.1013	-13.35	-5.25	16.91
-1.25	1.029	0.2353	-0.0882	-10.96	-0.69	7.599
-2.5	1.034	0.2397	-0.0882	-7.39	+3.62	-1.868
-3.75	1.035	0.2445	-0.0886	-3.30	5.26	-4.048
-5.0	1.030	0.2444	-0.0857	+1.15	5.91	-4.829

35

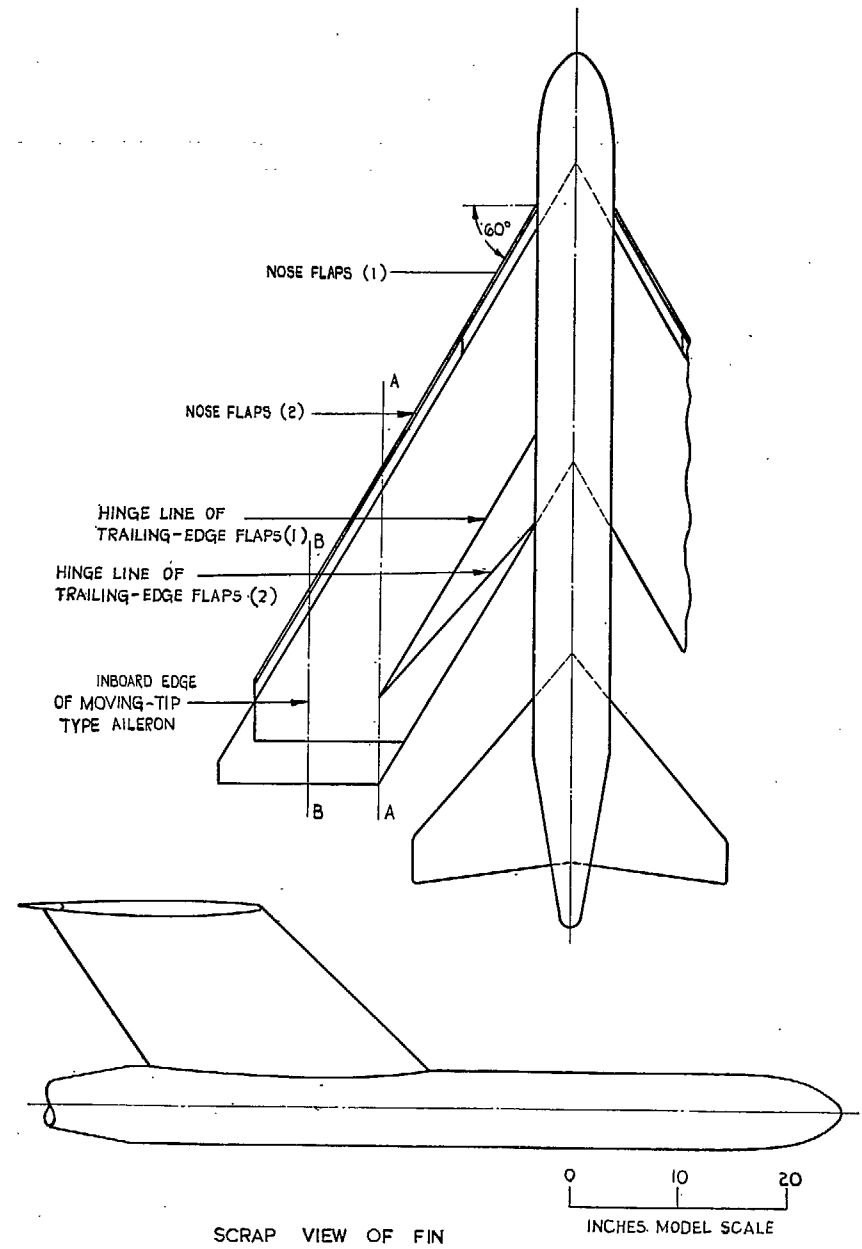


FIG. 1. View of underside of Model A.

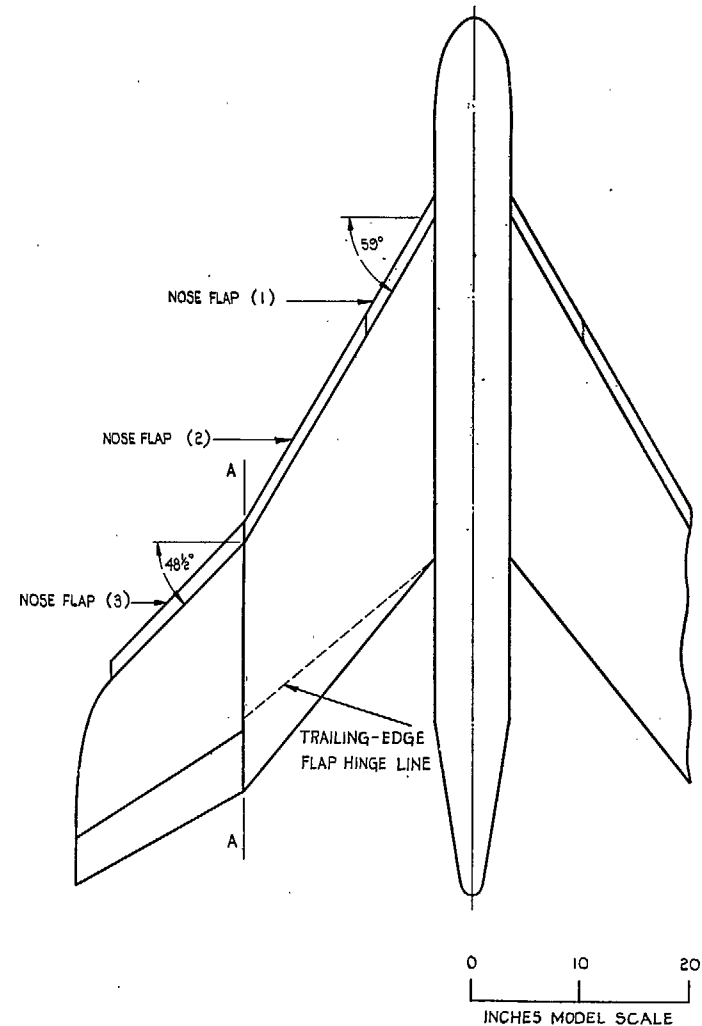
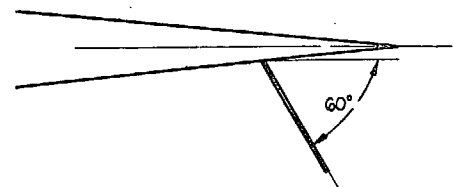
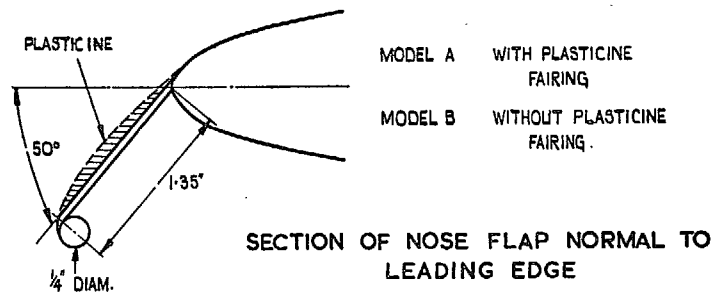


FIG. 2. Plan view of Model B.



36

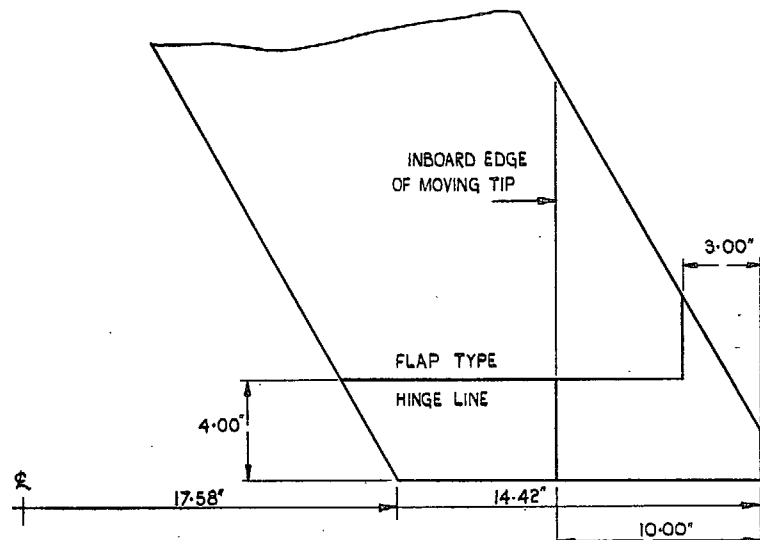


DIAGRAM OF AILERONS  
MODEL A

FIG. 3. Diagram of flaps.

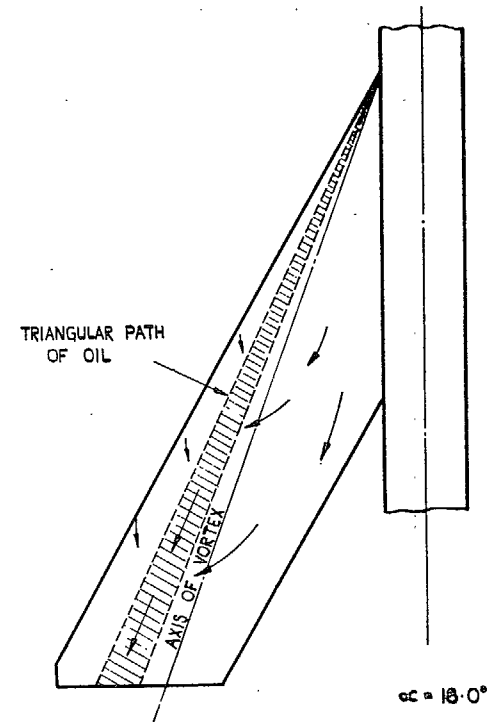


FIG. 4a.

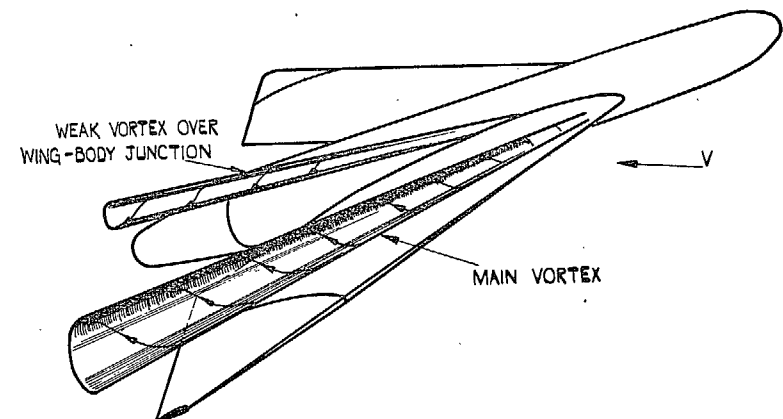
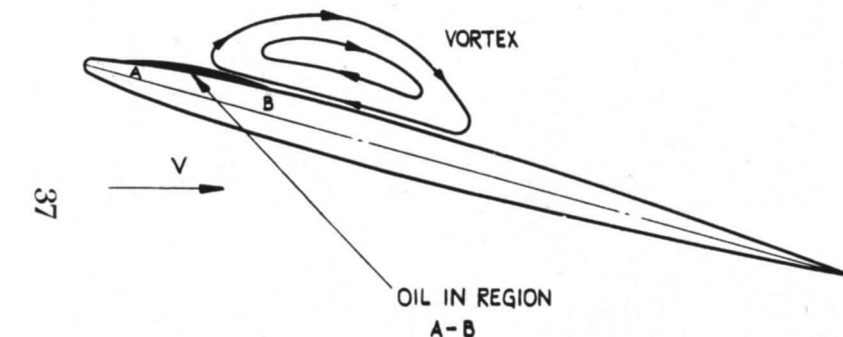


FIG. 4b.

Figs. 4a and 4b. Sketches of vortices.



37

FIG. 4c. Sketch showing probable position of vortex relative to oil.

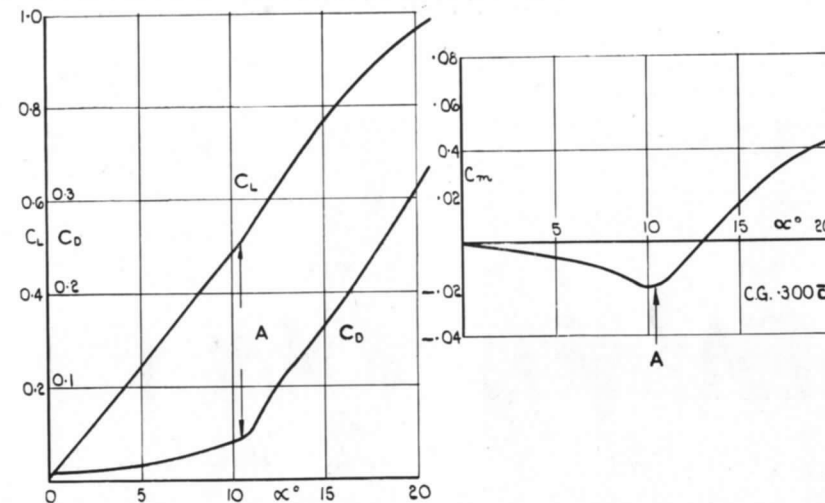


FIG. 5. Curves of  $C_L$ ,  $C_D$  and  $C_m$  vs.  $\alpha$  for Model A in tufted condition.

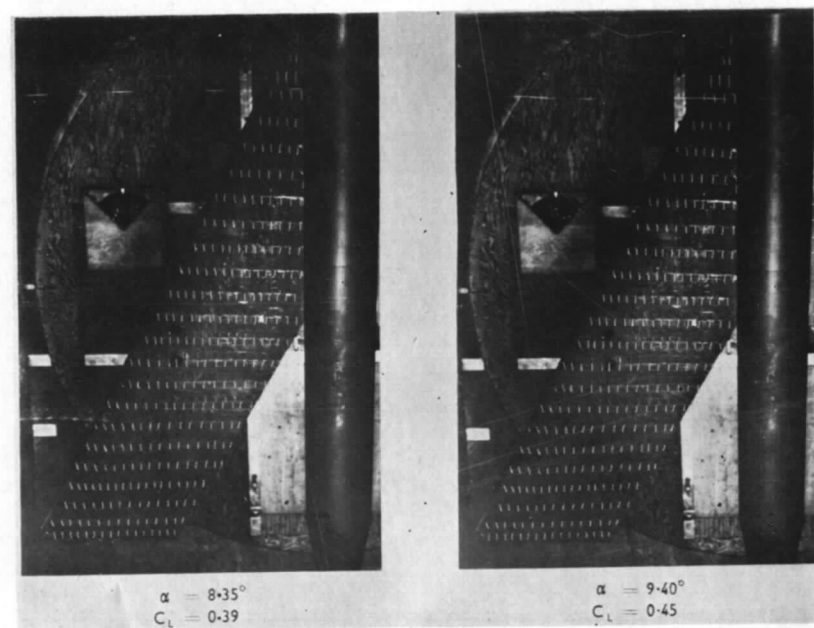


FIG. 5. Photographs of surface tufts on Model A, illustrating the development of the stall.

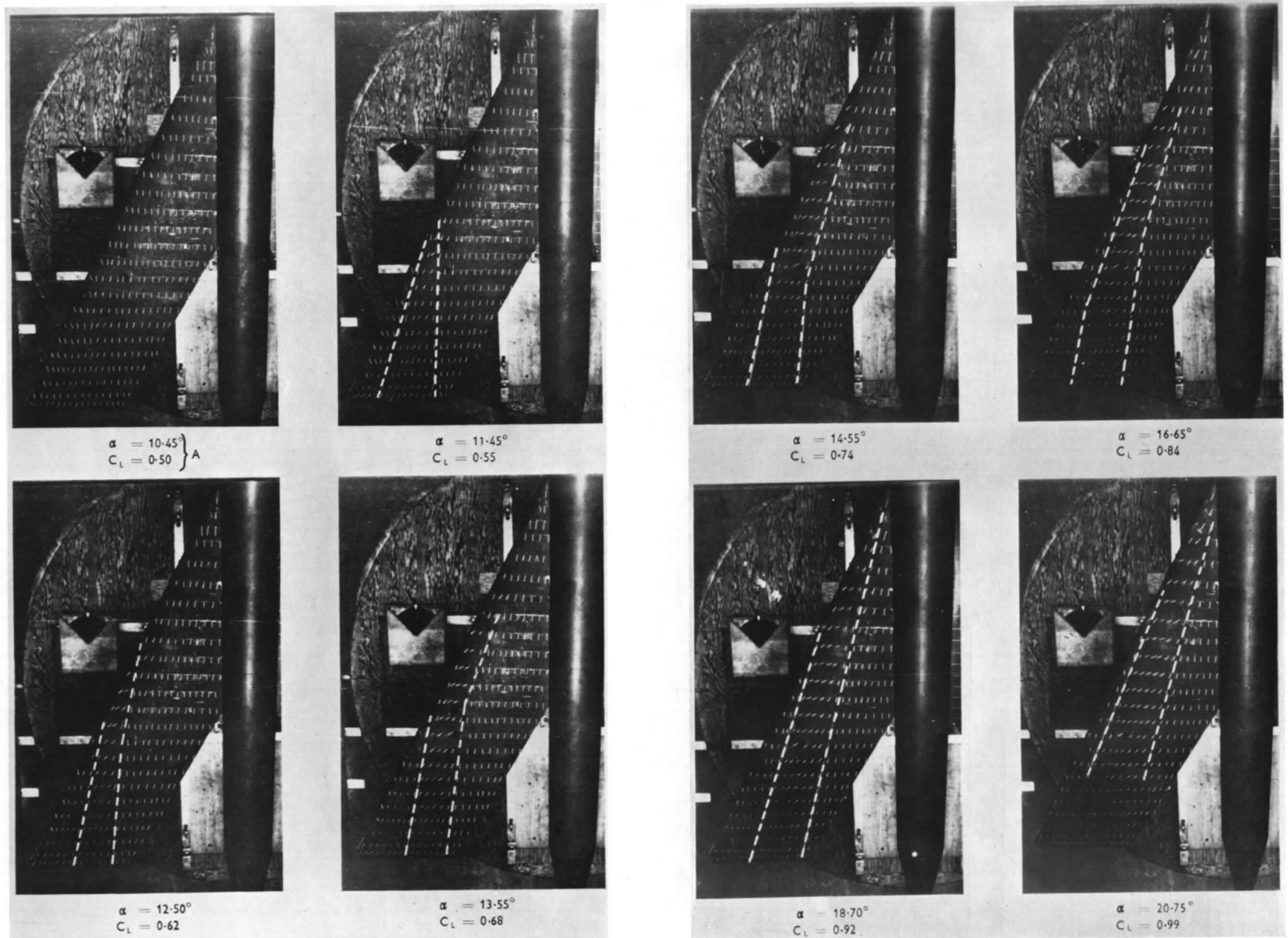


FIG. 5—continued. Photographs of surface tufts on Model A illustrating the development of the stall.

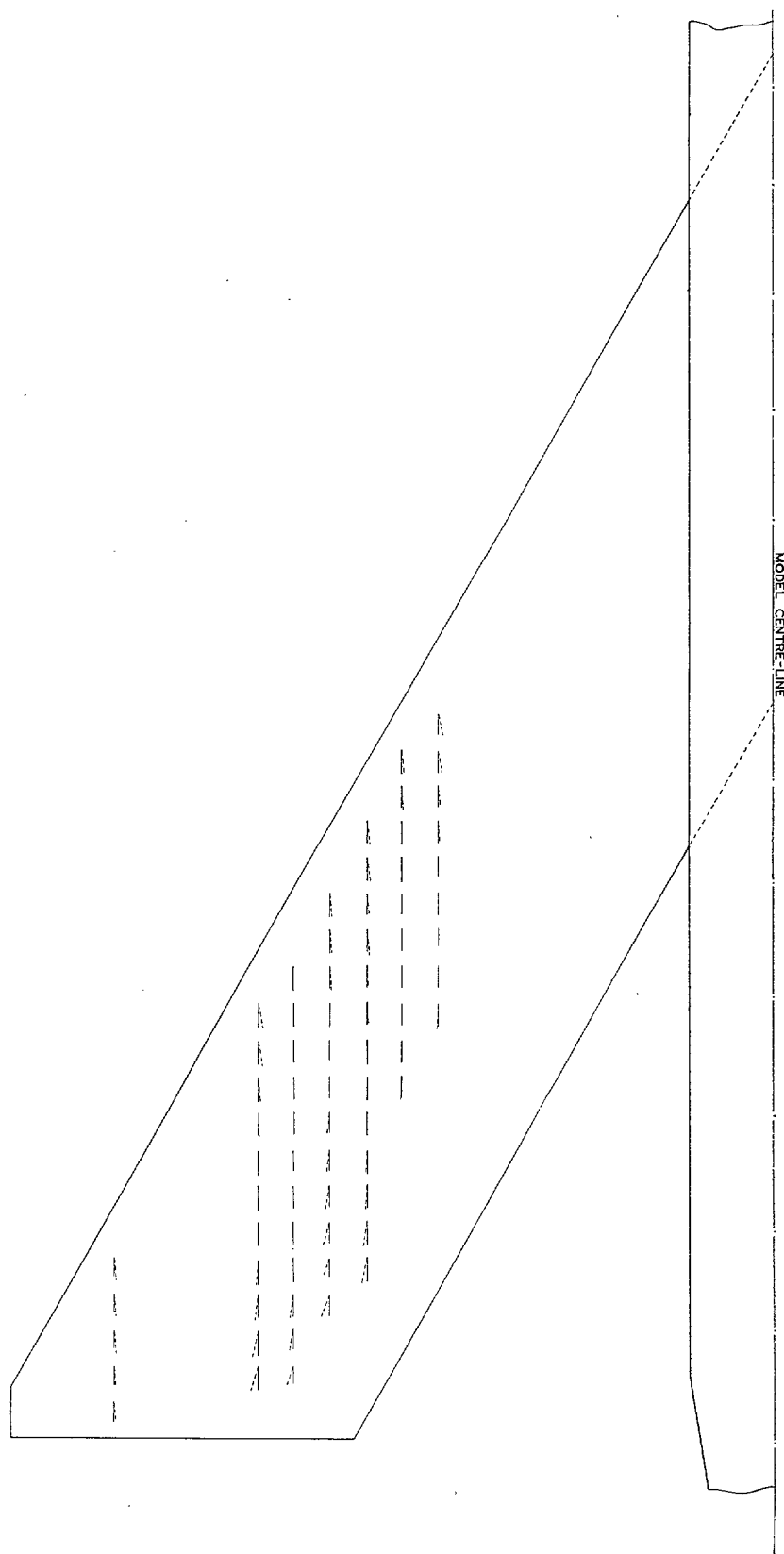


FIG. 6. Diagrams of tufts above the wing surface on Model A at  $\alpha = 9.40$  deg ( $C_L = 0.45$ ).

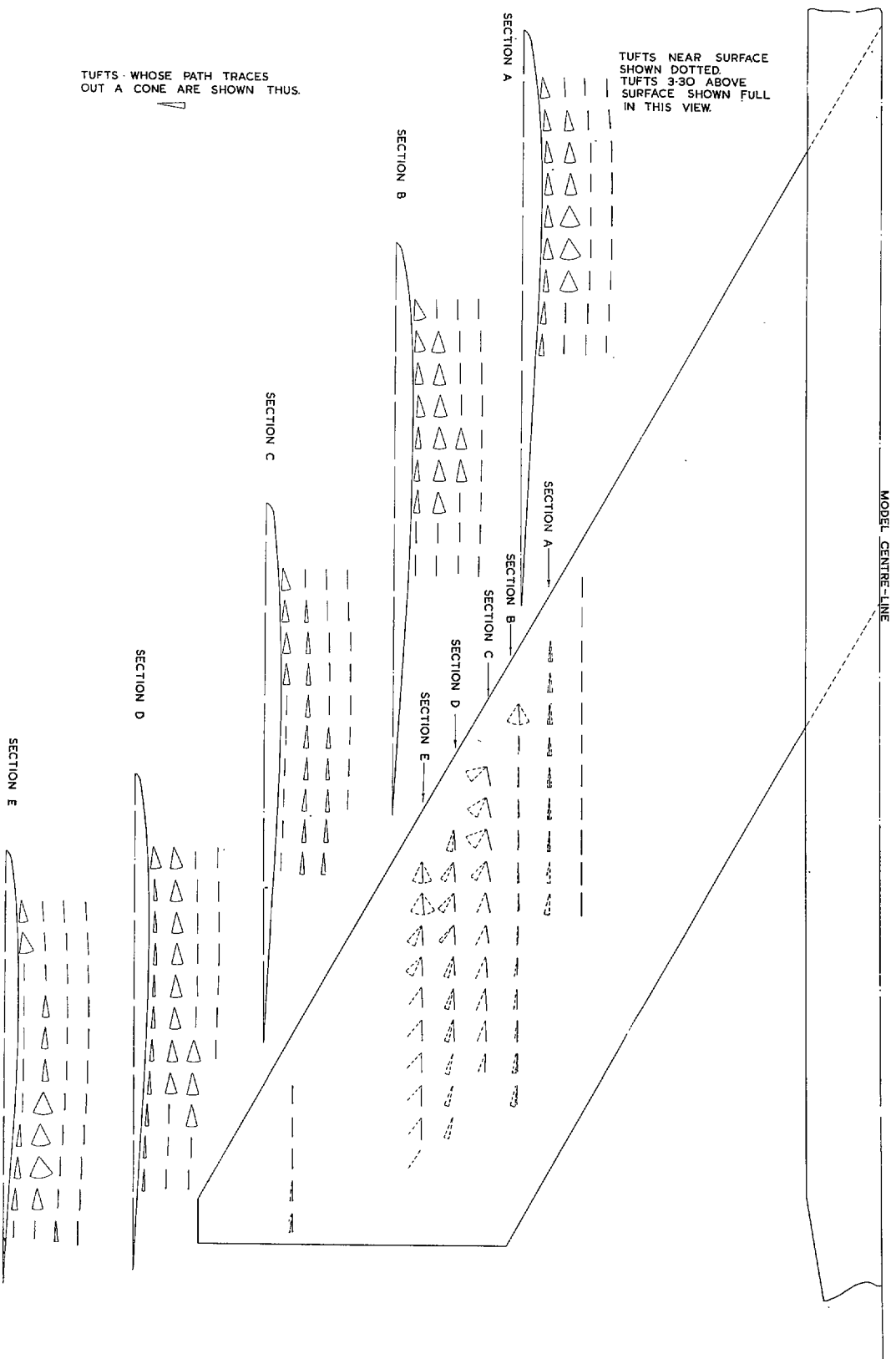


FIG. 7. Diagrams of tufts above wing surface on Model A at  $\alpha = 10\frac{1}{2}$  deg ( $C_L = 0.50$ ).

TUFTS WHOSE PATH TRACES  
OUT A CONE ARE SHOWN THUS

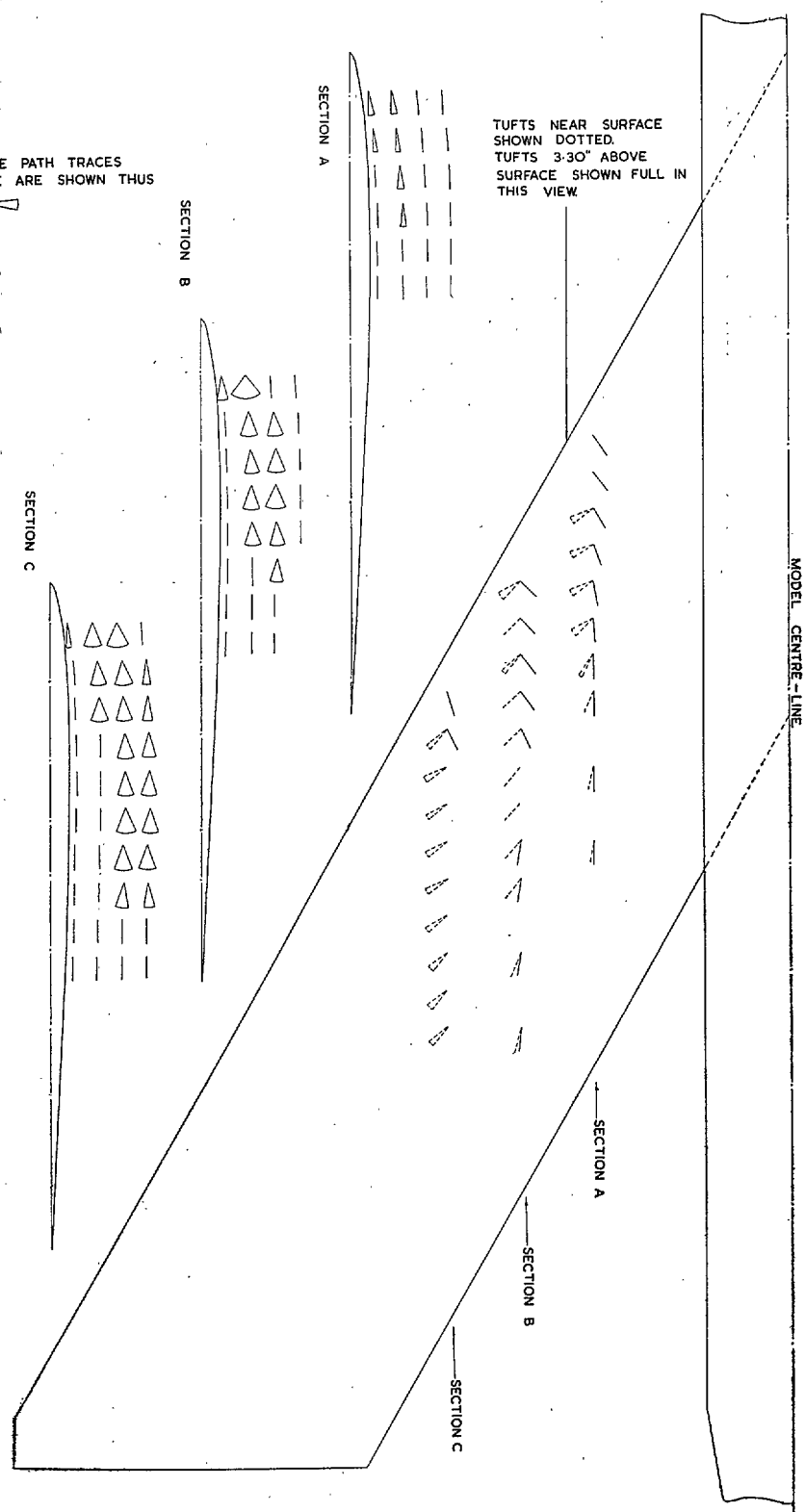


FIG. 8. Diagrams of tufts above the wing surface on Model A at  $\alpha = 18.70$  deg ( $C_L = 0.92$ ).

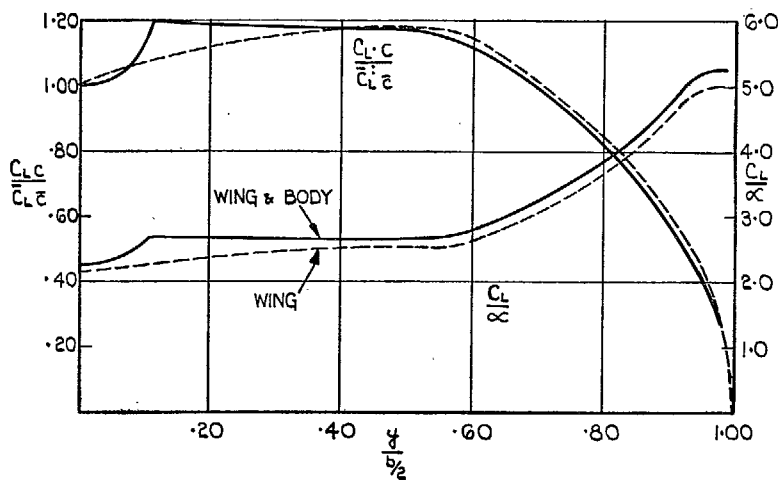


FIG. 9. Theoretical distribution of span loading on Model A.

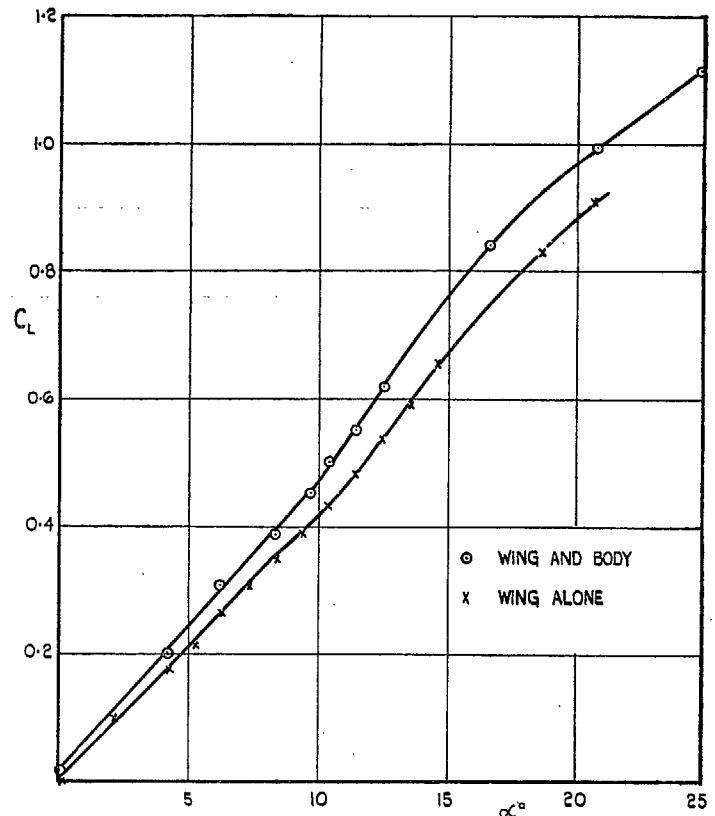


FIG. 10. Effect of body on lift Model A.

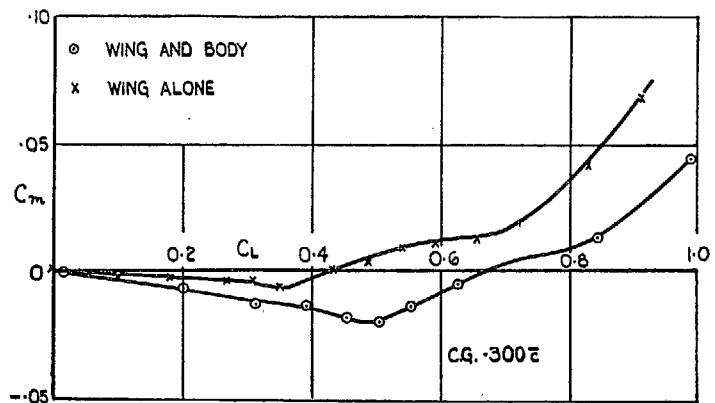


FIG. 11. Effect of Body on pitching moments, Model A.

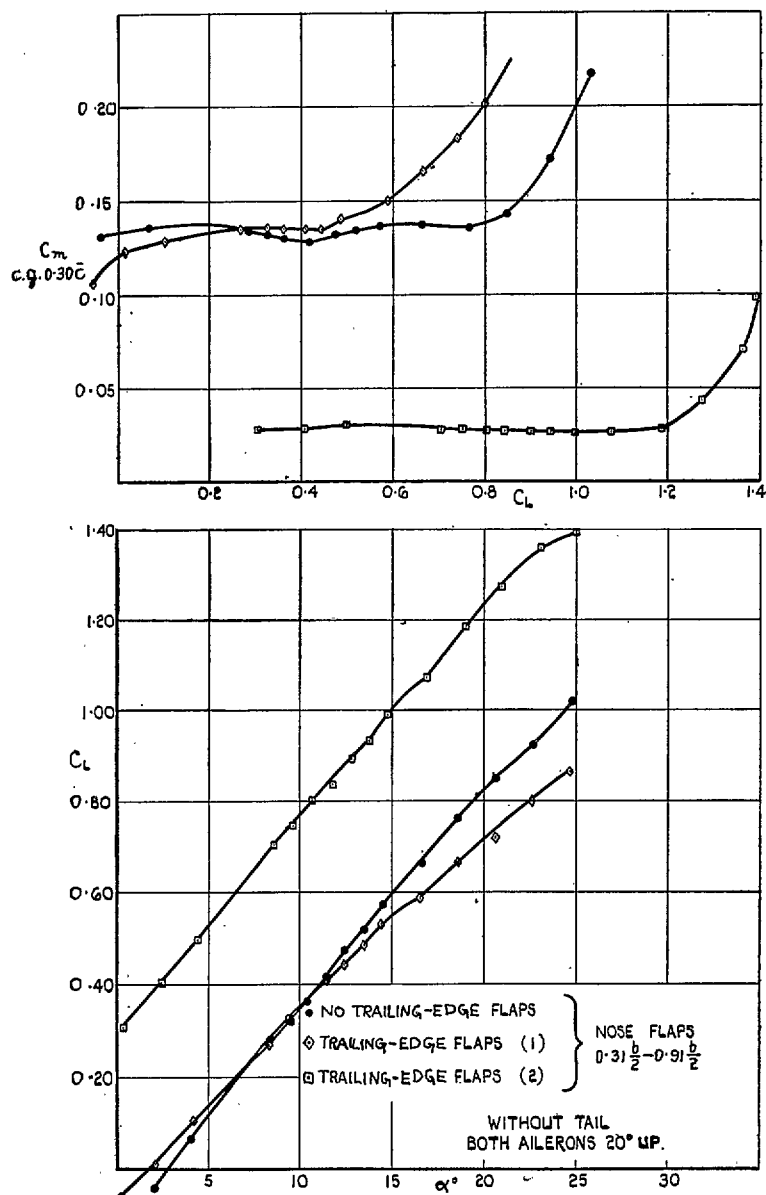


FIG. 12. Comparison of trailing-edge flaps (1) and (2). Model A.

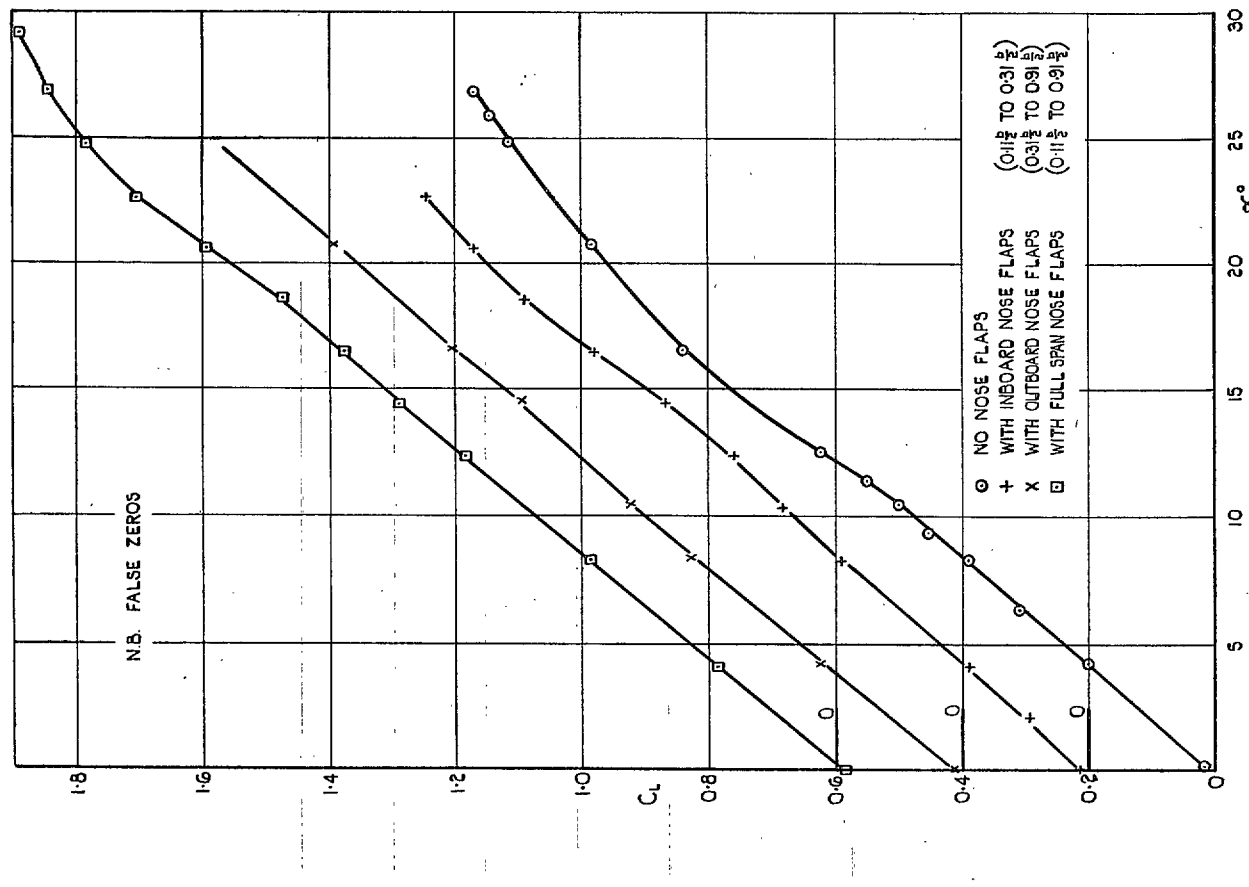


FIG. 13.  $C_L$  vs.  $\alpha$ . Effect of nose flaps. (Without trailing-edge flaps.) Model A.

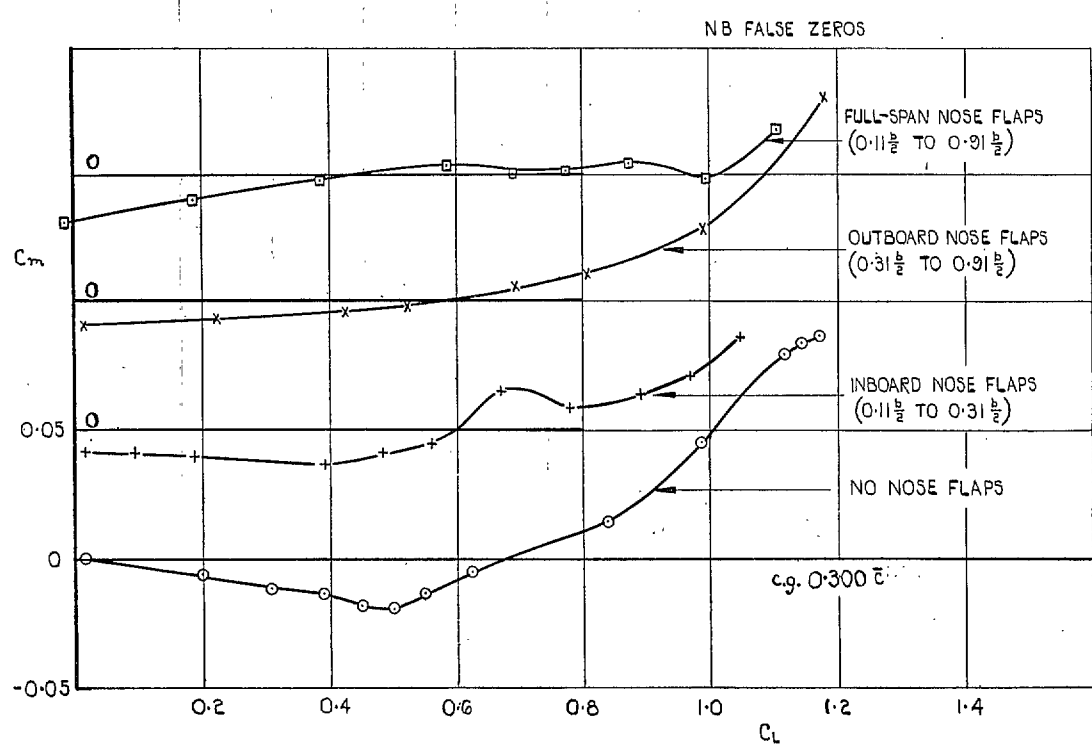


FIG. 14.  $C_m$  vs.  $C_L$ . Effect of nose flaps. (Without trailing-edge flaps.) Model A.

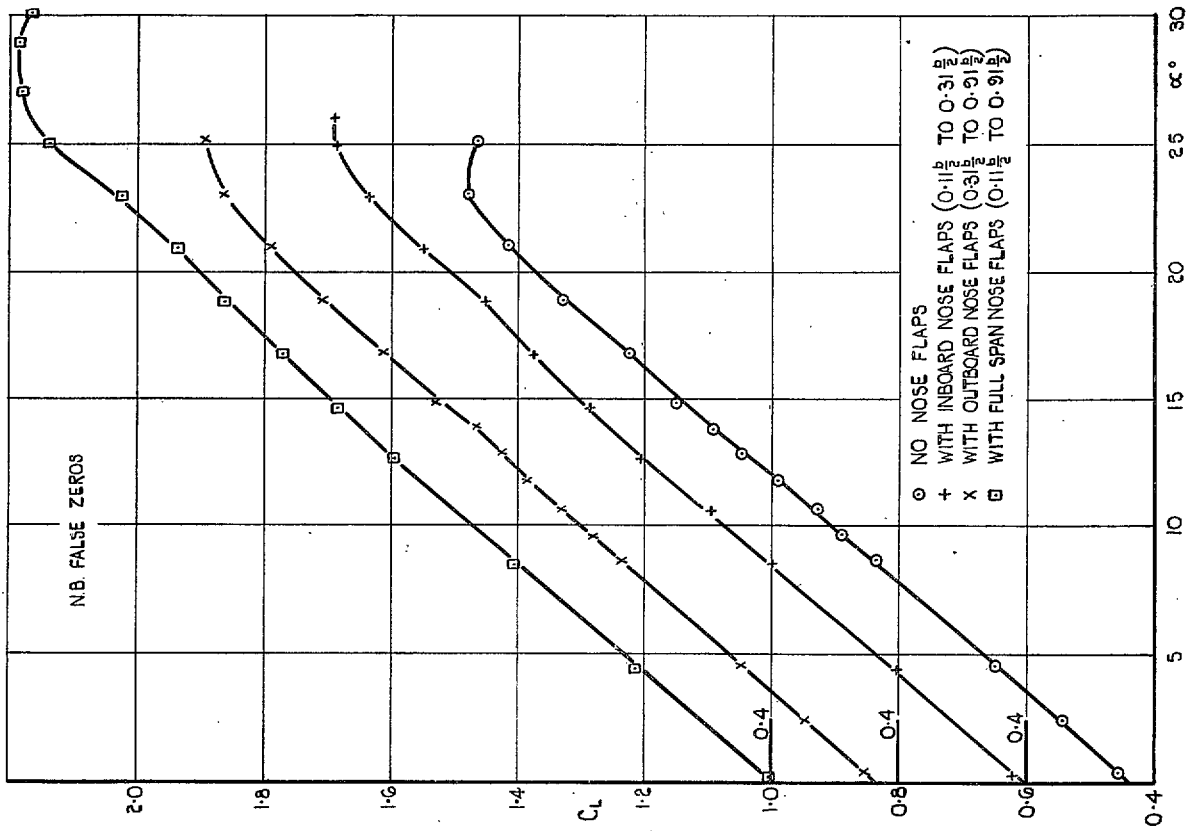
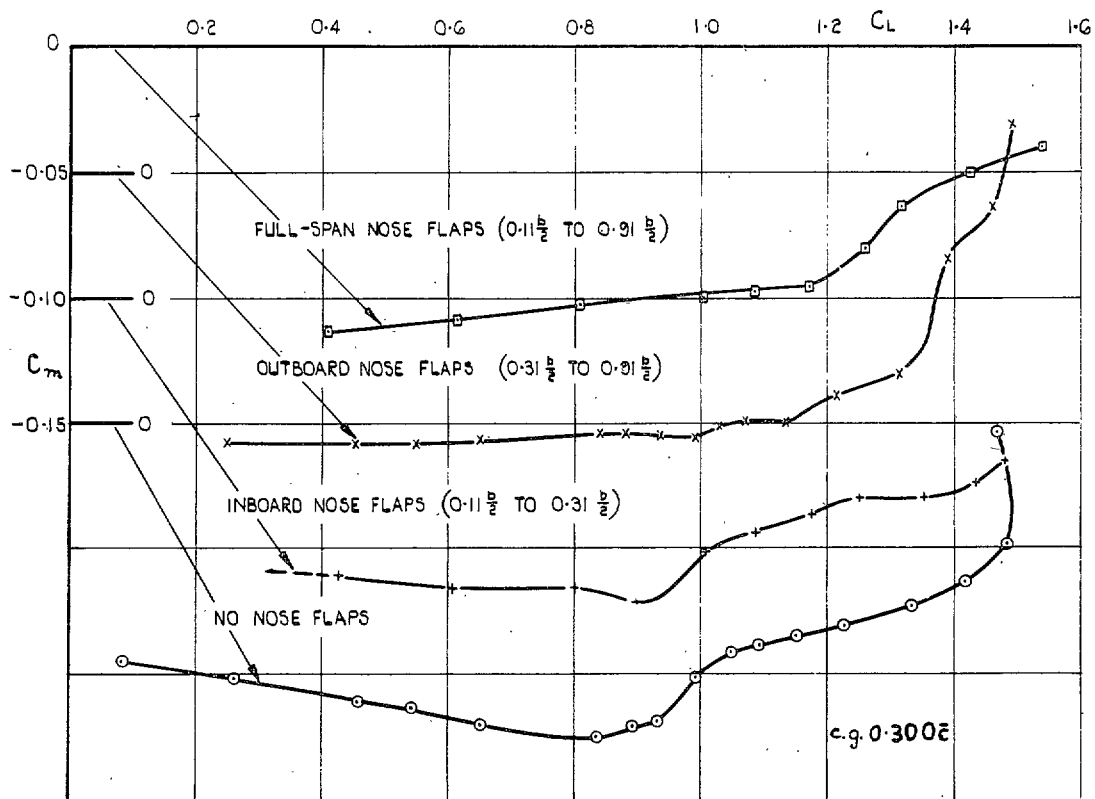


FIG. 15.  $C_L$  vs.  $\alpha$ . Effect of nose flaps. (With trailing-edge flaps (2).)  
Model A.



c.g. 0.300 $\bar{c}$

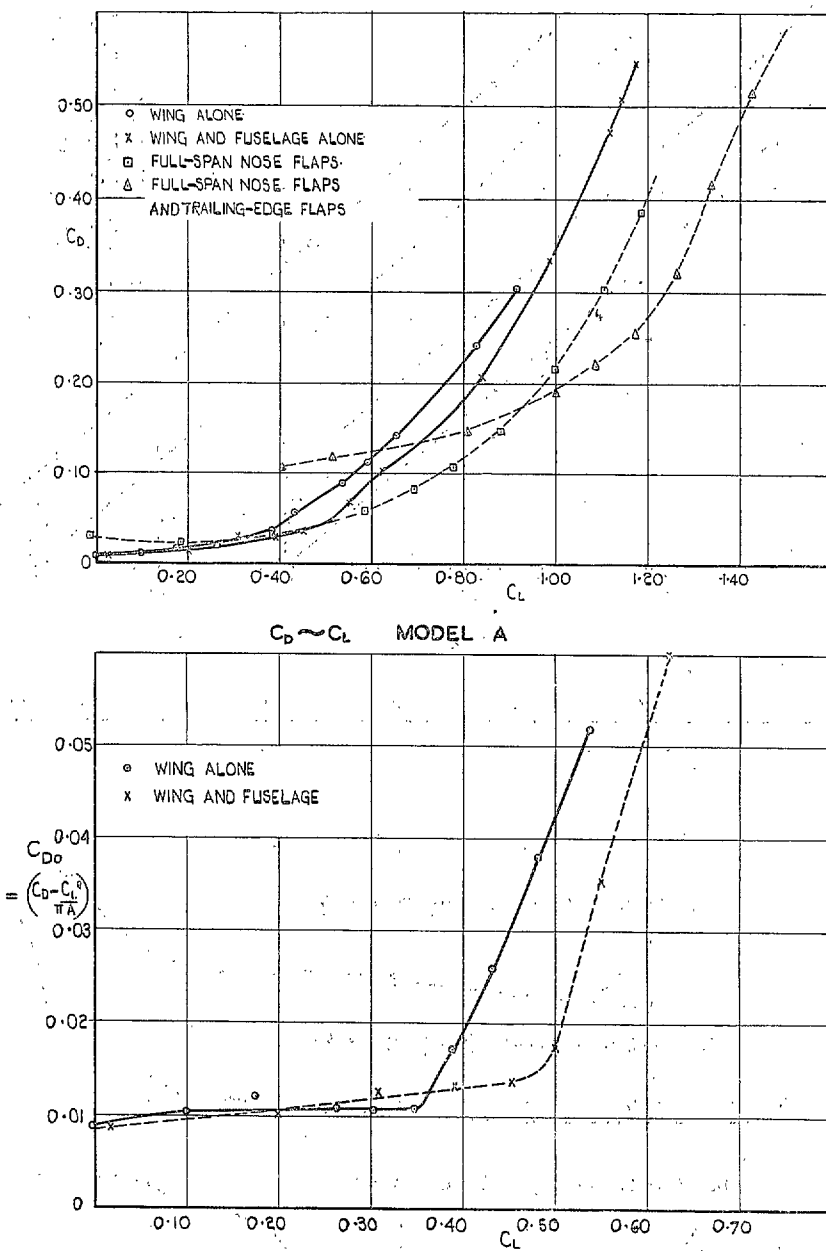


FIG. 17.  $C_{D_0}$  vs.  $C_L$ . Model A.

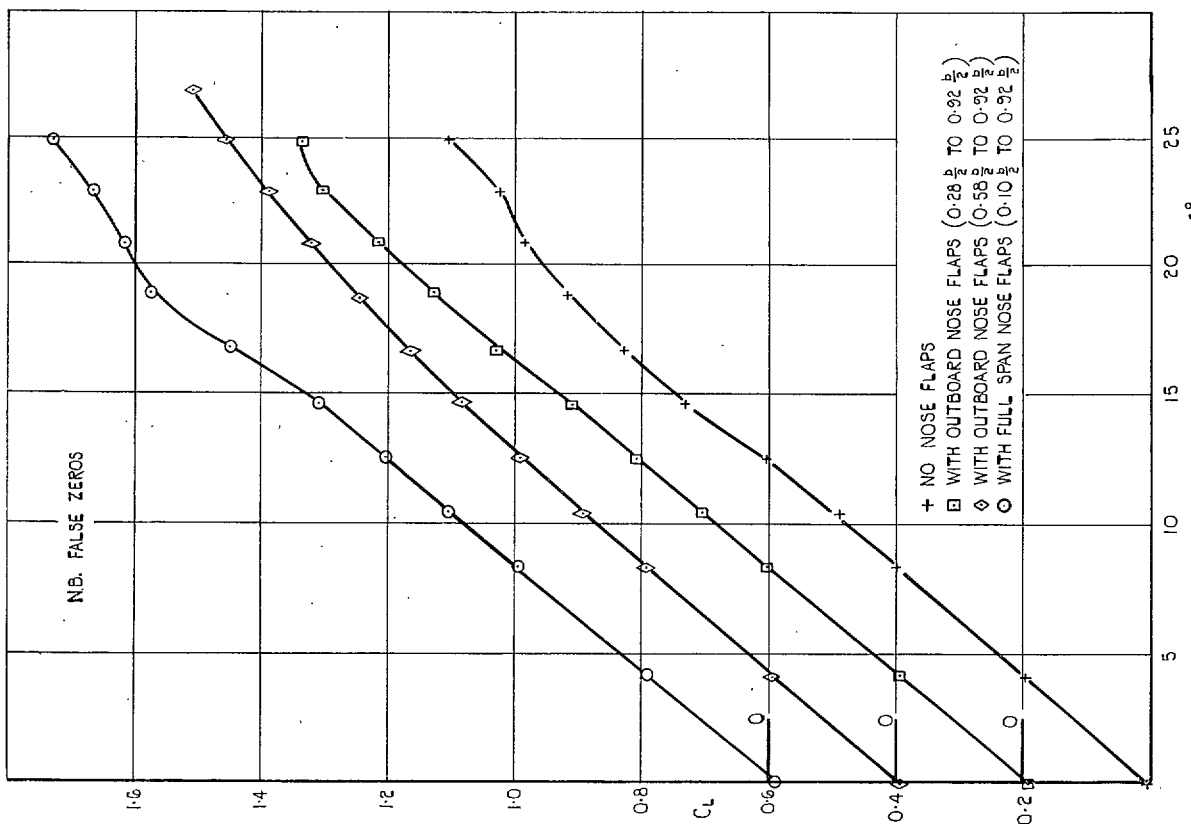


FIG. 18.  $C_L$  vs.  $\alpha$ . Effect of nose flaps. (Without trailing-edge flaps.)  
Model B.

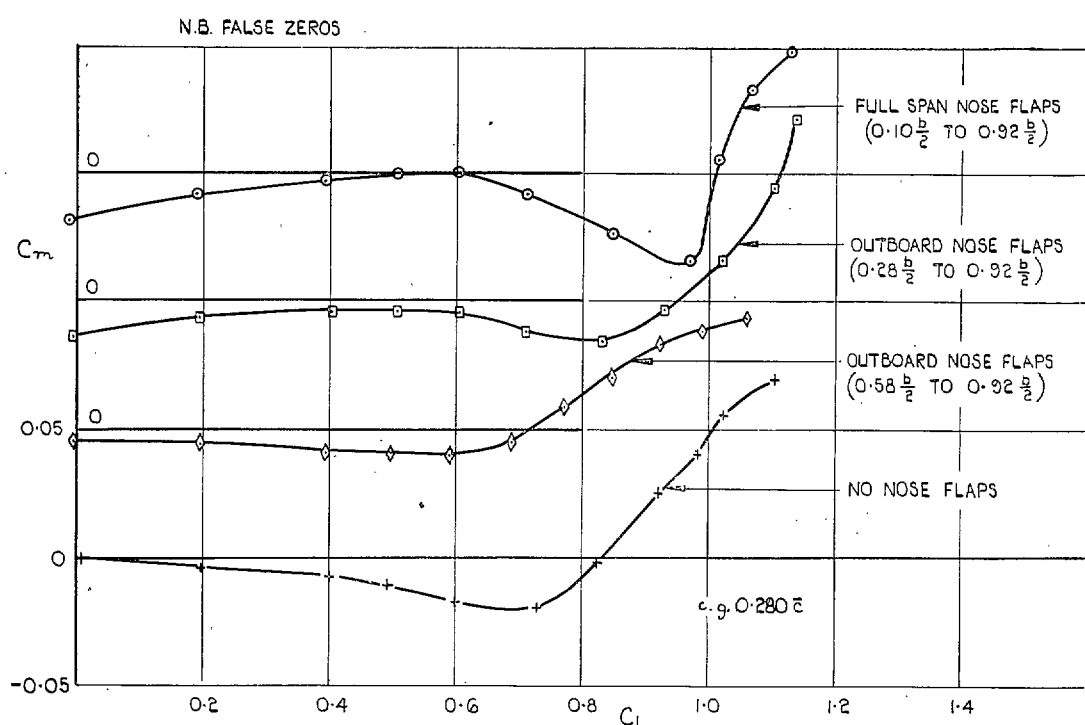


FIG. 19.  $C_m$  vs.  $C_L$ . Effect of nose flaps. (Without trailing-edge flaps.) Model B.

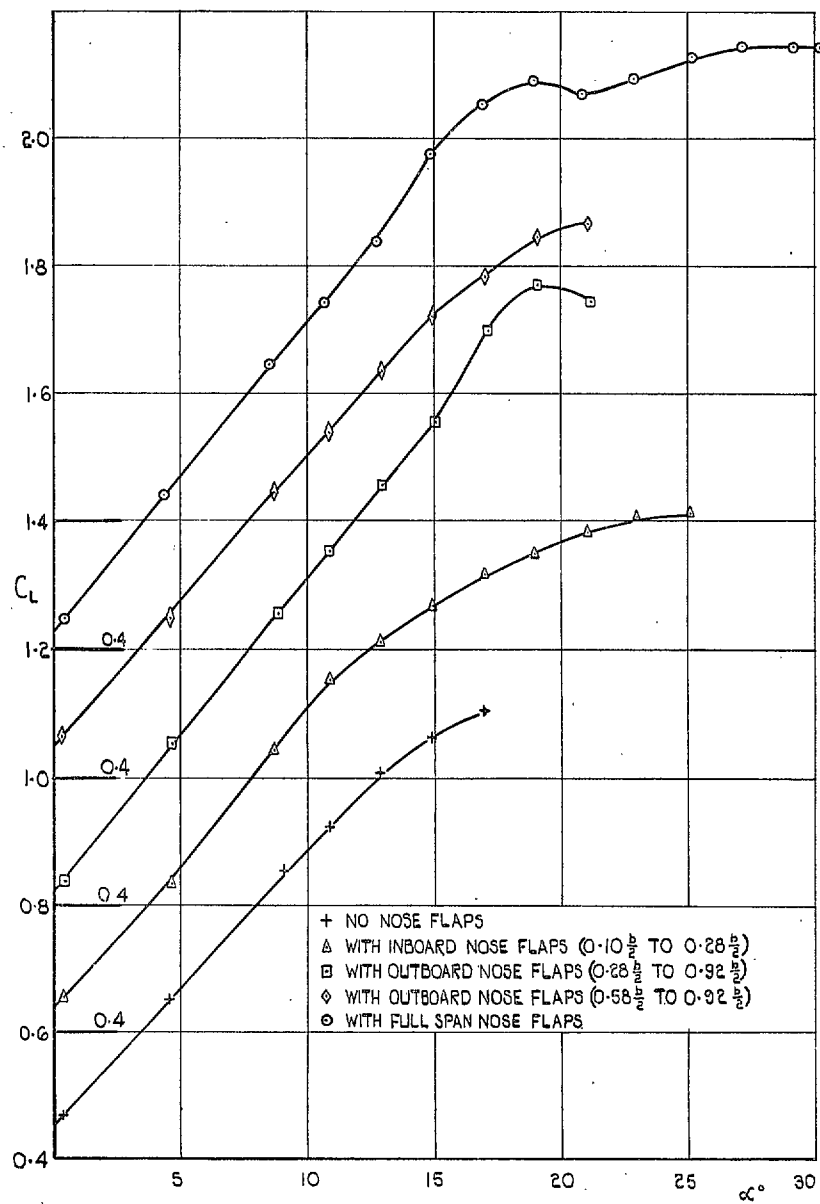


FIG. 20.  $C_L$  vs.  $\alpha$ . Effect of nose flaps. (With trailing-edge flaps.) Model B.

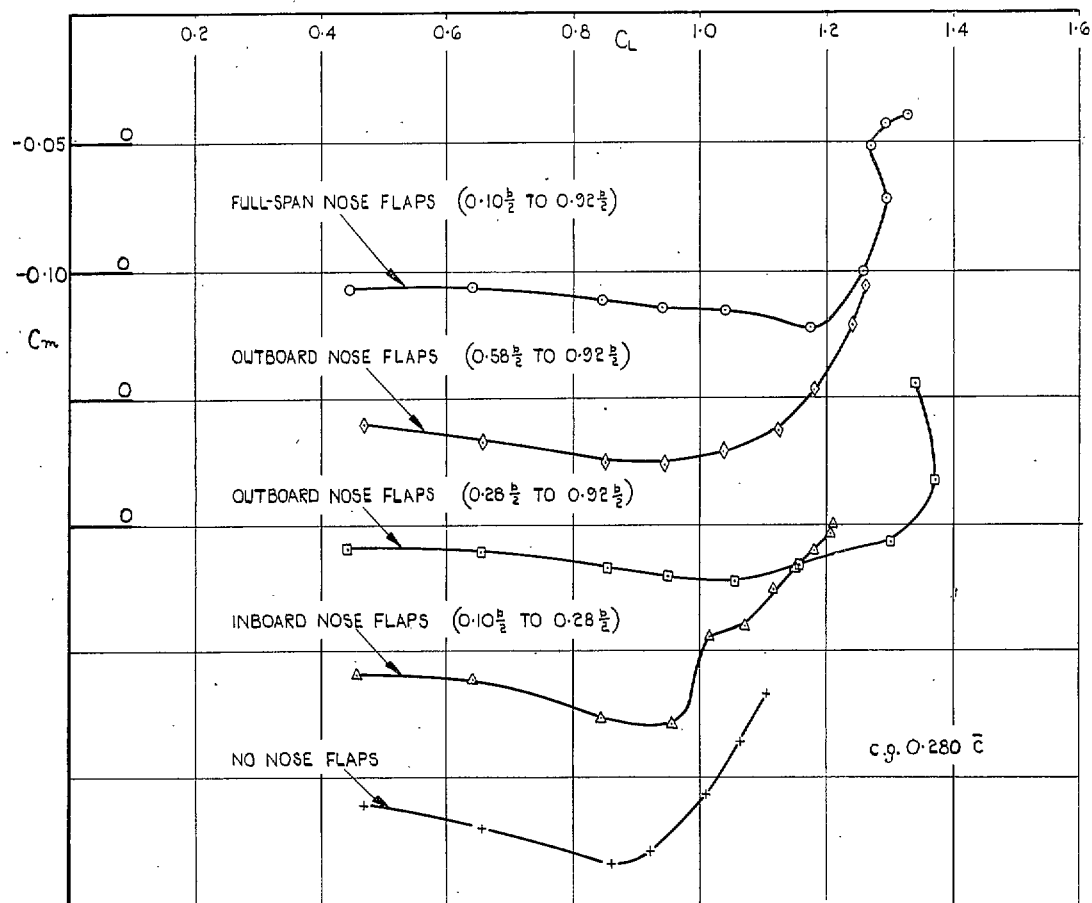


FIG. 21. Effect of nose flaps. (With trailing-edge flaps.) Model B.

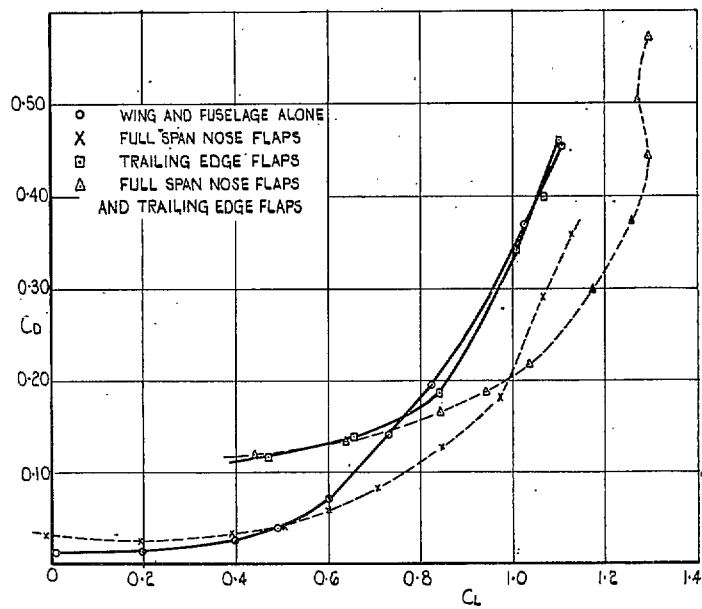


FIG. 22.  $C_D$  vs.  $C_L$ . Model B.

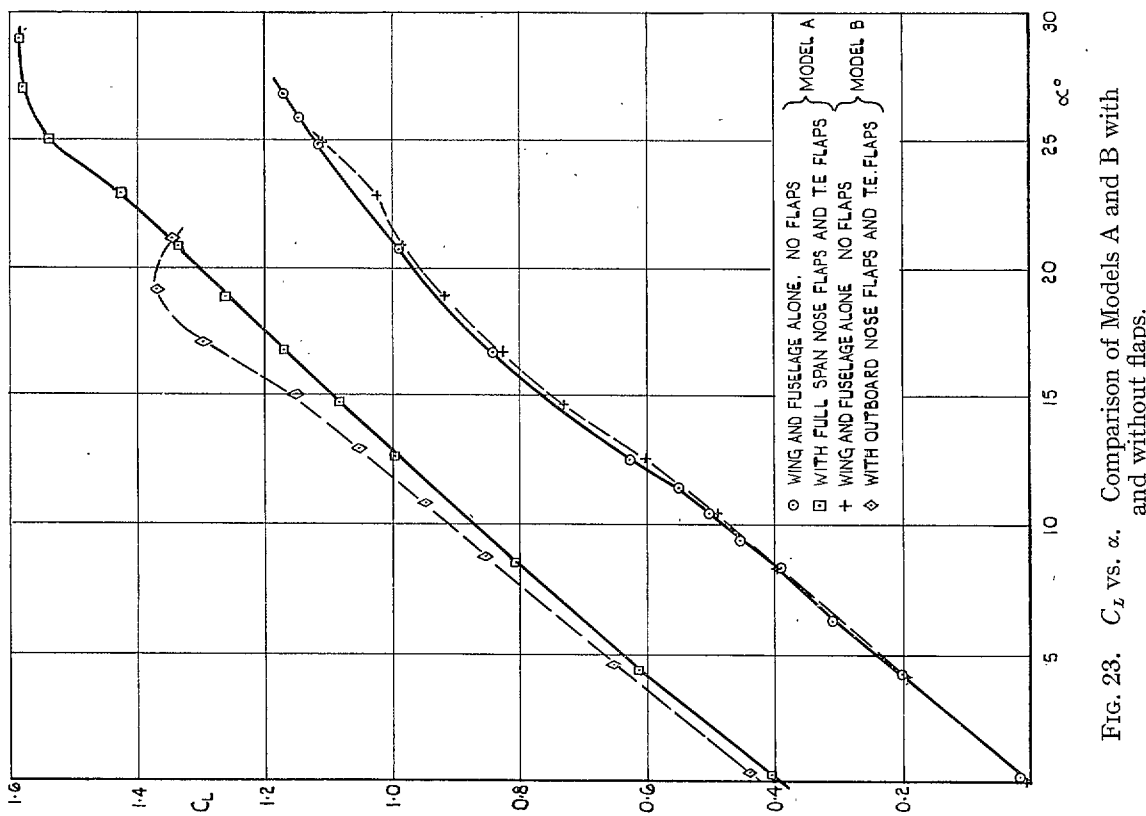


FIG. 23.  $C_L$  vs.  $\alpha$ . Comparison of Models A and B with and without flaps.

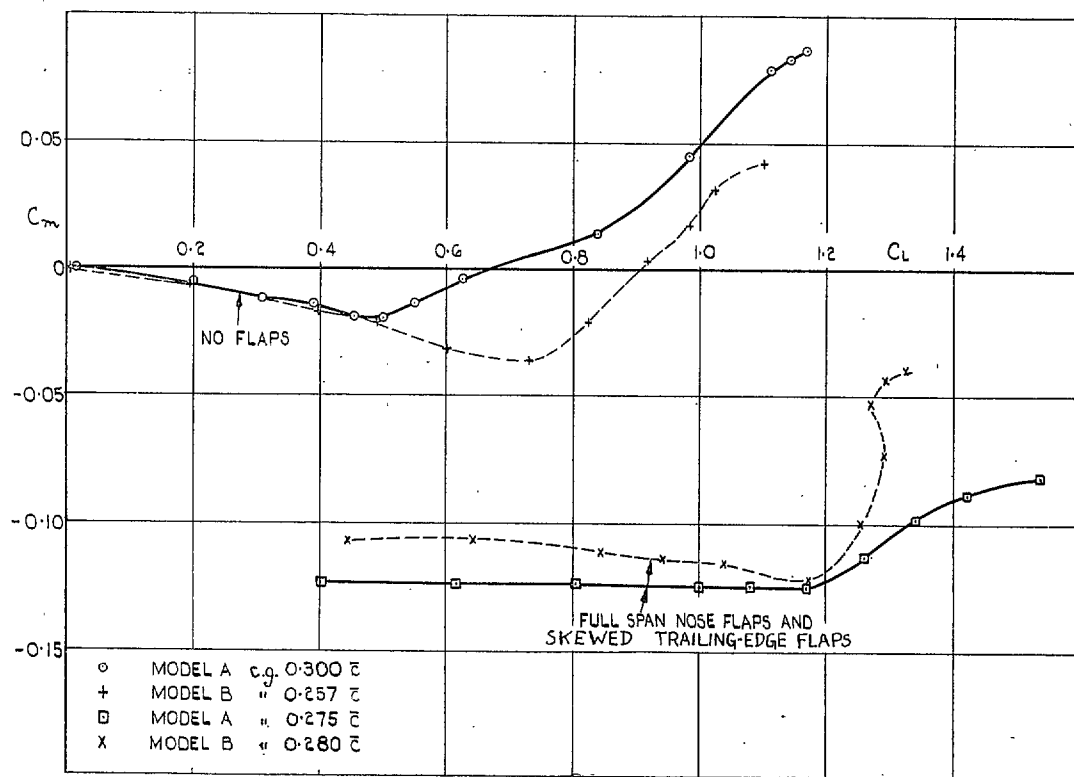


FIG. 24.  $C_m$  vs.  $C_L$ . Comparison of Models A and B with and without flaps.

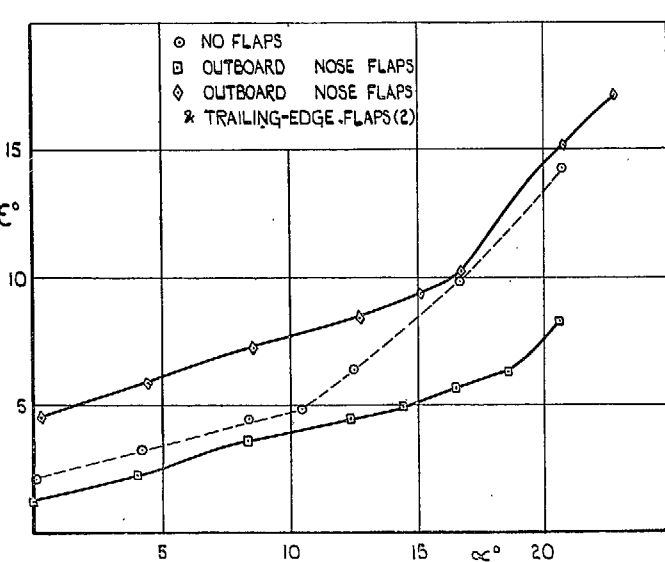
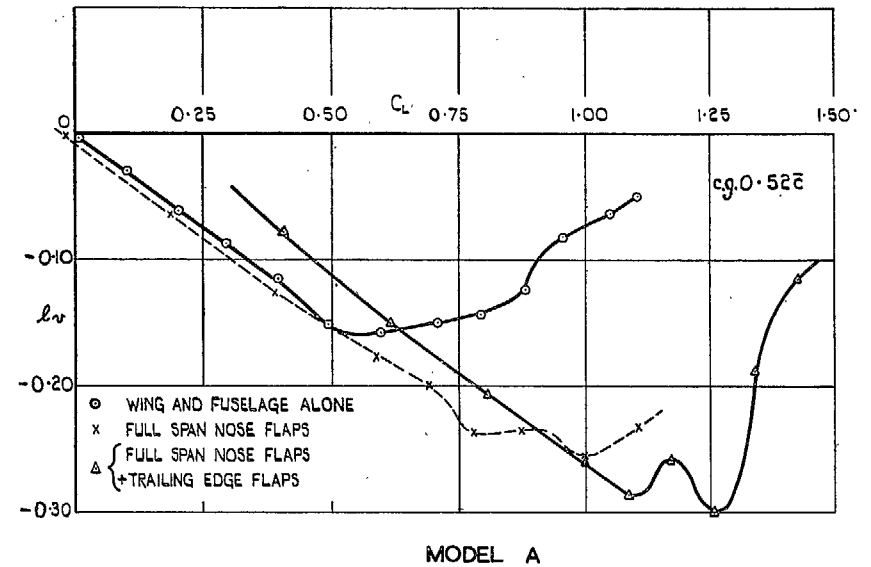
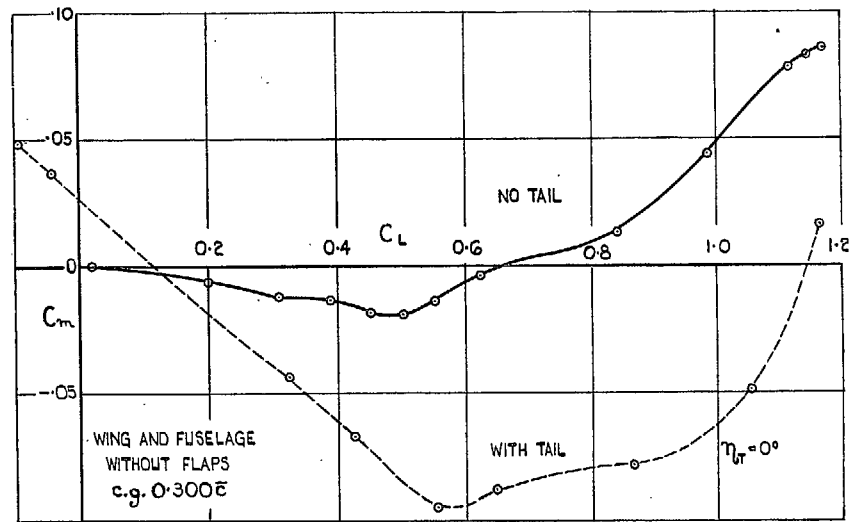


FIG. 26. Mean downwash at tailplane. Model A.

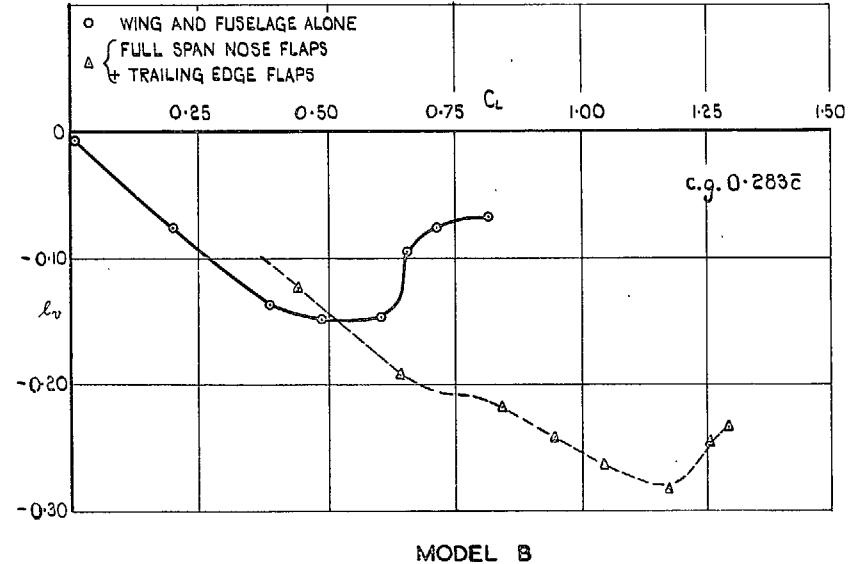
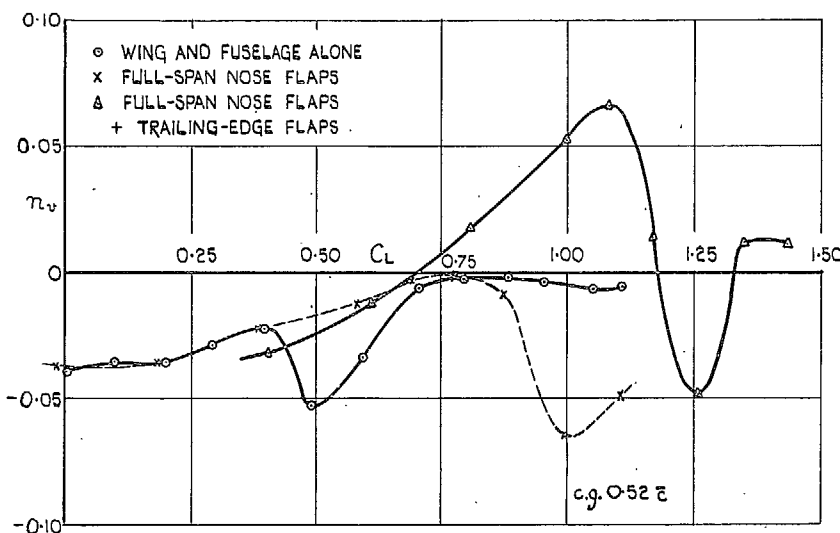
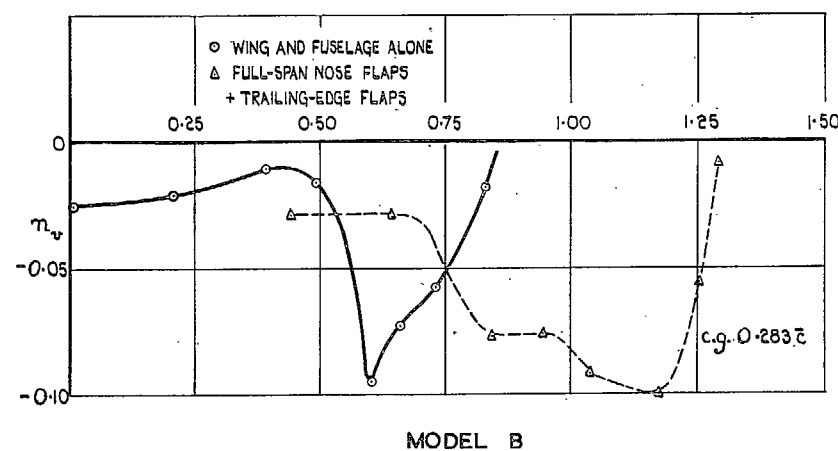


FIG. 27. Effect of flaps on  $l_v$ .



MODEL A



MODEL B

FIG. 28. Effect of flaps on  $n_v$ .

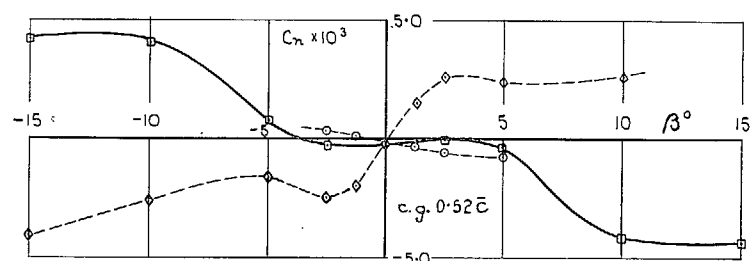
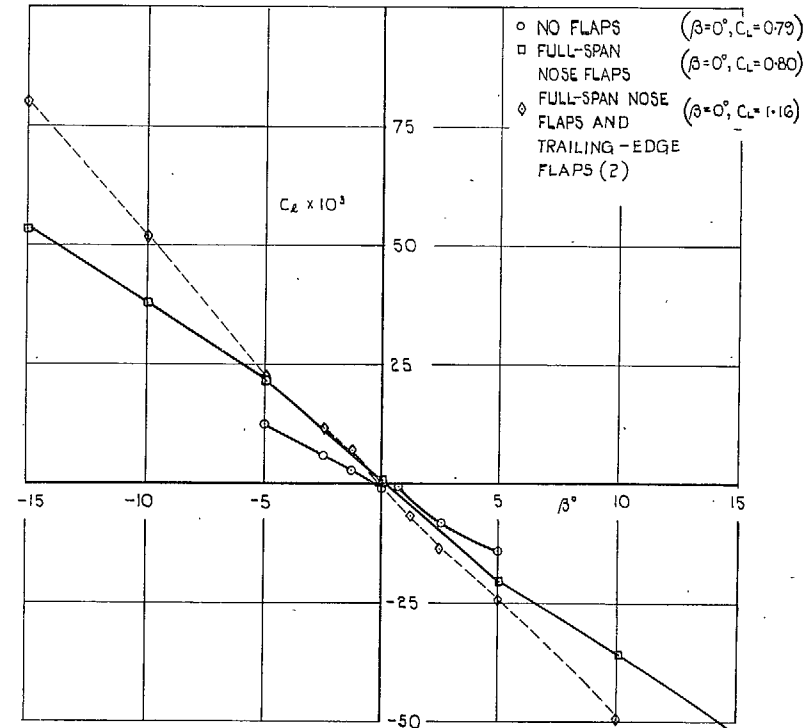


FIG. 29. Yawing and rolling moment vs. sideslip at  $\alpha = 16.6$  deg.  
Model A.

53

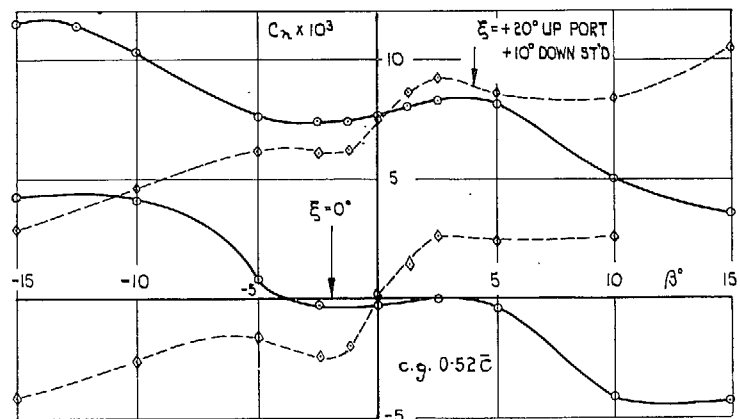
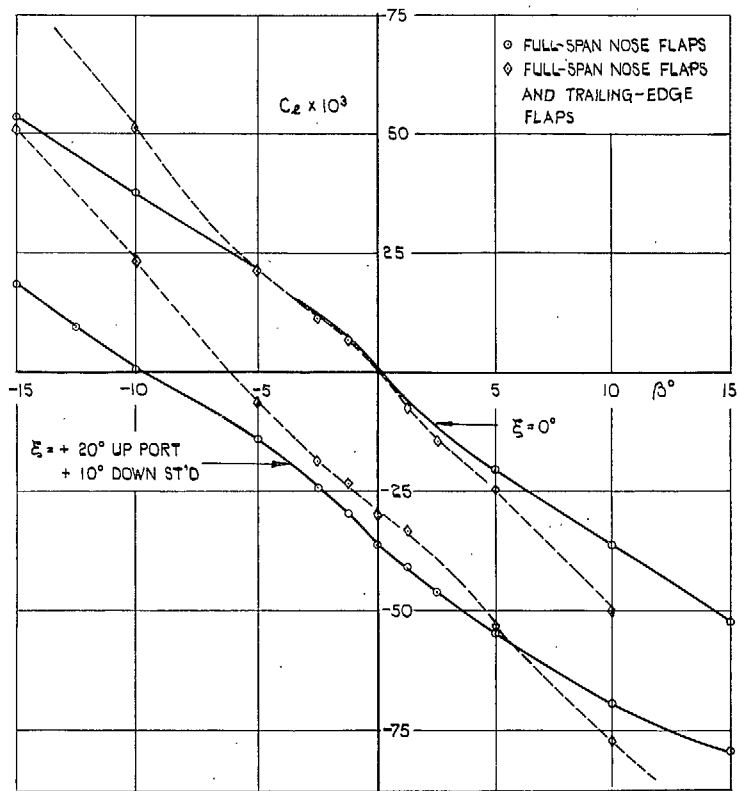


FIG. 30.  $C_L$  and  $C_d$  vs.  $\beta$  deg. Effect of aileron deflection at  $\alpha = 16.6$  deg. Model A.

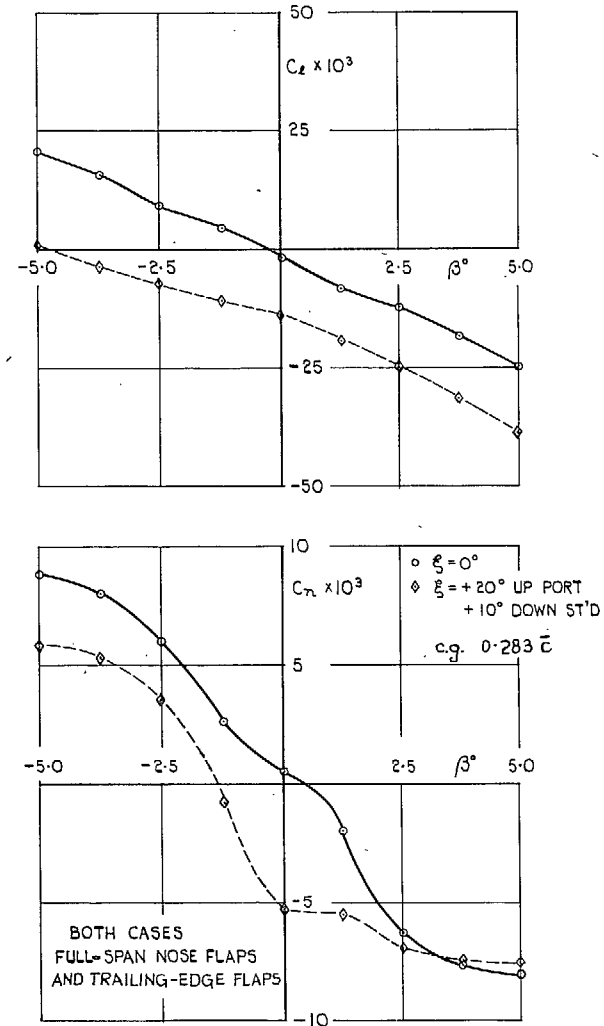


FIG. 31.  $C_L$  and  $C_d$  vs.  $\beta$  deg. Effect of aileron deflection at  $\alpha = 12.7$  deg. Model B.

54

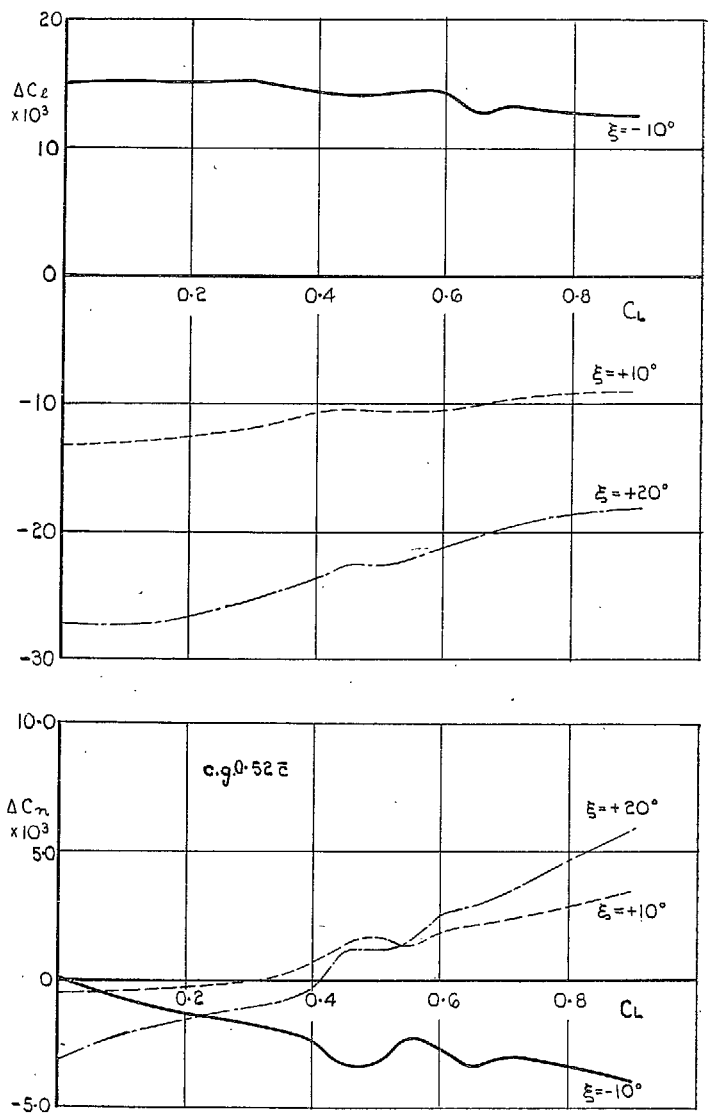


FIG. 32. Model A. Wing and fuselage alone.  
(Flap-type aileron.)

FIGS. 32 and 33. Effect of aileron deflection (port only) on rolling and yawing moments.

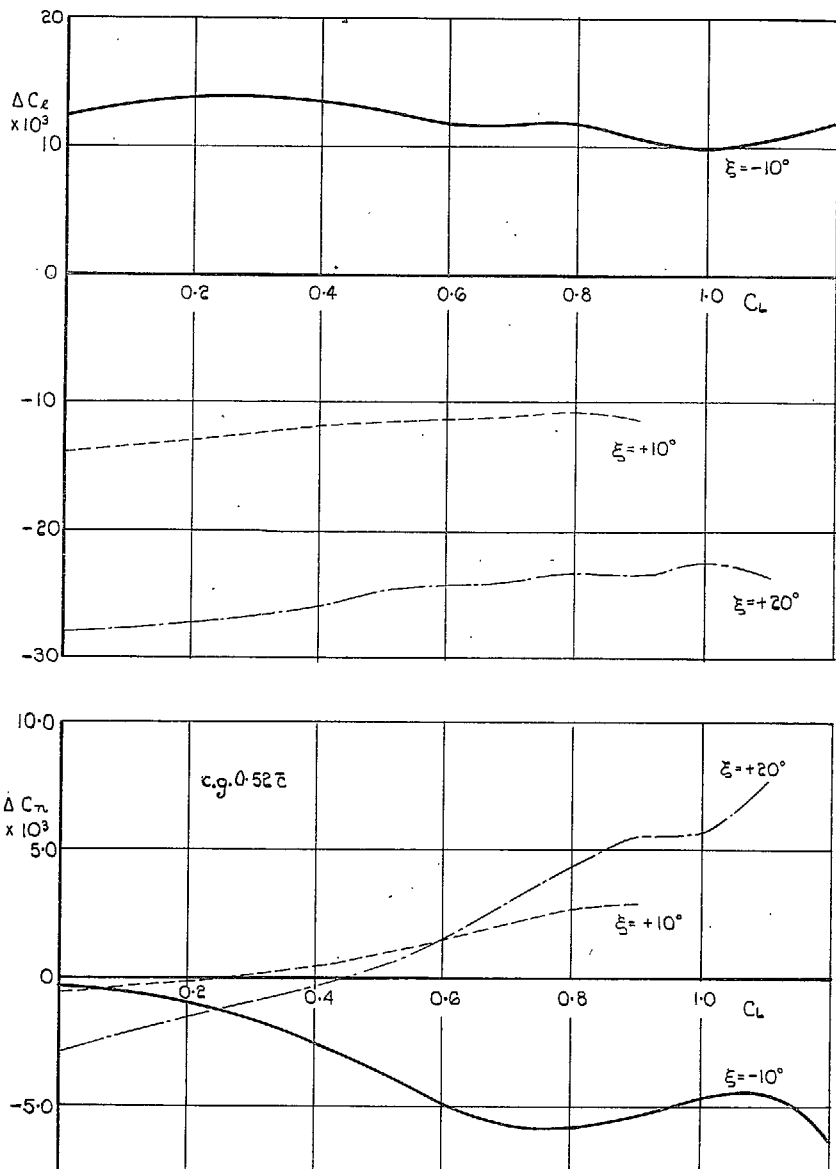


FIG. 33. Model A. Full-span nose flaps. (Flap-type aileron.)

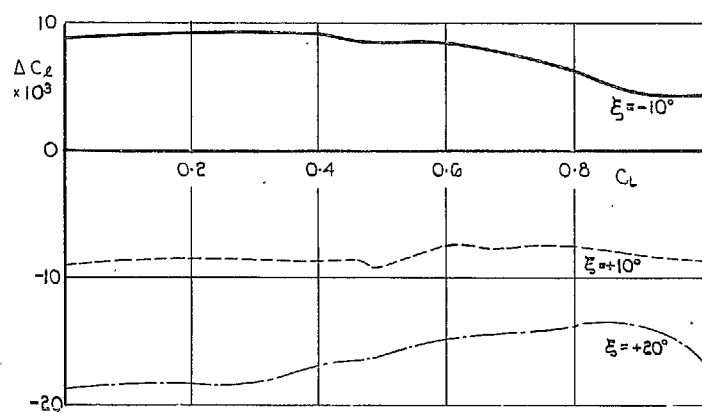
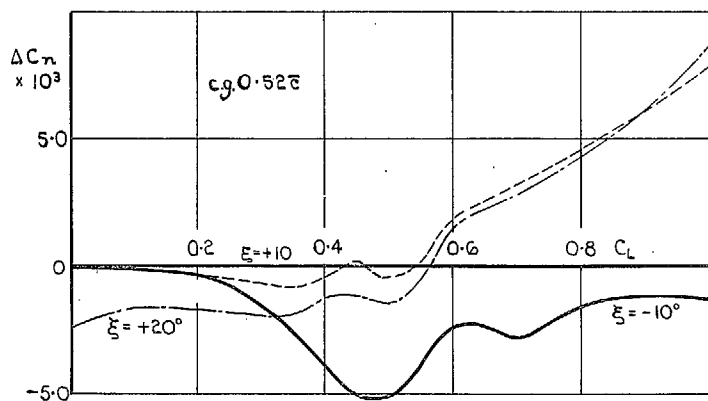


FIG. 34. Model A. Wing and fuselage alone.  
(Moving-tip type aileron.)



FIGS. 34 and 35. Effect of aileron deflection (port only) on rolling and yawing moments.

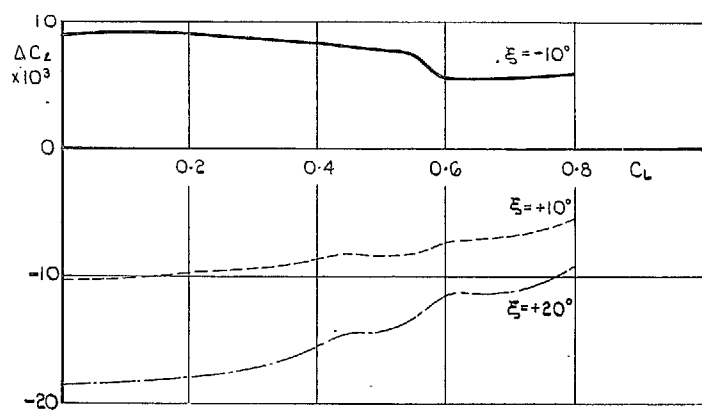
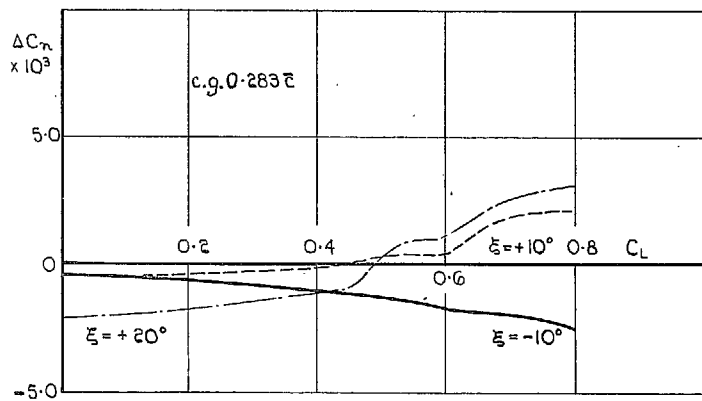


FIG. 35. Model B. Wing and fuselage alone.  
(Flap-type aileron.)



# Publications of the Aeronautical Research Council

## **ANNUAL TECHNICAL REPORTS OF THE AERONAUTICAL RESEARCH COUNCIL (BOUNDED VOLUMES)**

- 1939 Vol. I. Aerodynamics General, Performance, Airscrews, Engines. 50s. (51s. 9d.)  
           Vol. II. Stability and Control, Flutter and Vibration, Instruments, Structures, Seaplanes, etc.  
           63s. (64s. 9d.)
- 1940 Aero and Hydrodynamics, Aerofoils, Airscrews, Engines, Flutter, Icing, Stability and Control  
           Structures, and a miscellaneous section. 50s. (51s. 9d.)
- 1941 Aero and Hydrodynamics, Aerofoils, Airscrews, Engines, Flutter, Stability and Control  
           Structures. 63s. (64s. 9d.)
- 1942 Vol. I. Aero and Hydrodynamics, Aerofoils, Airscrews, Engines. 75s. (76s. 9d.)  
           Vol. II. Noise, Parachutes, Stability and Control, Structures, Vibration, Wind Tunnels.  
           47s. 6d. (49s. 3d.)
- 1943 Vol. I. Aerodynamics, Aerofoils, Airscrews. 80s. (81s. 9d.)  
           Vol. II. Engines, Flutter, Materials, Parachutes, Performance, Stability and Control, Structures.  
           90s. (92s. 6d.)
- 1944 Vol. I. Aero and Hydrodynamics, Aerofoils, Aircraft, Airscrews, Controls. 84s. (86s. 3d.)  
           Vol. II. Flutter and Vibration, Materials, Miscellaneous, Navigation, Parachutes, Performance,  
           Plates and Panels, Stability, Structures, Test Equipment, Wind Tunnels.  
           84s. (86s. 3d.)
- 1945 Vol. I. Aero and Hydrodynamics, Aerofoils. 130s. (132s. 6d.)  
           Vol. II. Aircraft, Airscrews, Controls. 130s. (132s. 6d.)  
           Vol. III. Flutter and Vibration, Instruments, Miscellaneous, Parachutes, Plates and Panels,  
           Propulsion. 130s. (132s. 3d.)  
           Vol. IV. Stability, Structures, Wind Tunnels, Wind Tunnel Technique. 130s. (132s. 3d.)

### **Annual Reports of the Aeronautical Research Council—**

1937 2s. (2s. 2d.)      1938 1s. 6d. (1s. 8d.)      1939-48 3s. (3s. 3d.)

### **Index to all Reports and Memoranda published in the Annual Technical Reports, and separately—**

April, 1950 - - - - R. & M. 2600 2s. 6d. (2s. 8d.)

### **Author Index to all Reports and Memoranda of the Aeronautical Research Council—**

1909—January, 1954      R. & M. No. 2570 15s. (15s. 6d.)

### **Indexes to the Technical Reports of the Aeronautical Research Council—**

December 1, 1936—June 30, 1939	R. & M. No. 1850	1s. 3d. (1s. 5d.)
July 1, 1939—June 30, 1945	R. & M. No. 1950	1s. (1s. 2d.)
July 1, 1945—June 30, 1946	R. & M. No. 2050	1s. (1s. 2d.)
July 1, 1946—December 31, 1946	R. & M. No. 2150	1s. 3d. (1s. 5d.)
January 1, 1947—June 30, 1947	R. & M. No. 2250	1s. 3d. (1s. 5d.)

### **Published Reports and Memoranda of the Aeronautical Research Council—**

Between Nos. 2251—2349	R. & M. No. 2350	1s. 9d. (1s. 11d.)
Between Nos. 2351—2449	R. & M. No. 2450	2s. (2s. 2d.)
Between Nos. 2451—2549	R. & M. No. 2550	2s. 6d. (2s. 8d.)
Between Nos. 2551—2649	R. & M. No. 2650	2s. 6d. (2s. 8d.)

*Prices in brackets include postage*

### **HER MAJESTY'S STATIONERY OFFICE**

York House, Kingsway, London, W.C.2; 423 Oxford Street, London, W.1; 13a Castle Street, Edinburgh 2;  
 39 King Street, Manchester 2; 2 Edmund Street, Birmingham 3; 109 St. Mary Street, Cardiff; Tower Lane, Bristol, 1;  
 80 Chichester Street, Belfast, or through any bookseller.